Research Article

Systemic co-administration of low dose oxytocin and glucagon like peptide-1 additively decreases food intake and body weight

Yuko Maejima[1,2,3], Shoko Yokota[1], Shizu Hidema[1], Katsuhiko Nishimori[2], Heidi de Wet[3], Kenju Shimomura[1, 2]

[1]*Department of Bioregulation and Pharmacological Medicine, Fukushima Medical University School of Medicine, Fukushima-shi, 960-1295, Fukushima, Japan*

[2]*Departments of Obesity and Inflammation Research, Fukushima Medical University School of Medicine, Fukushima-shi, 960-1295, Fukushima, Japan*

[3]*Department of Physiology, Anatomy and Genetics, Sherrington Building, University of Oxford, United Kingdom*

Address for Correspondence: Yuko Maejima or Kenju Shimomura

Address: Department of Bioregulation and Pharmacological Medicine, Fukushima Medical University School of Medicine, Fukushima-shi, 960-1295, Fukushima, Japan.

Telephone: +81-24-547-1152

E-mail: maejimay@fmu.ac.jp, shimomur@fmu.ac.jp

Running head: Oxytocin and glucagon like peptide-1 additively decrease food intake

Keywords: glucagon like peptide-1, obesity, oxytocin, oxytocin neurons

Abstract

Introduction: GLP-1 receptor agonists are the number one drug prescribed for the treatment of obesity and type 2 diabetes. These drugs are not, however, without side-effects and in an effort to maximize therapeutic effect while minimizing adverse effects, gut hormone co-agonists received considerable attention as new drug targets in the fight against obesity. Numerous previous reports identified the neuropeptide oxytocin (OXT) as a promising anti-obesity drug. The aim of this study is to evaluate OXT as a possible co-agonist for GLP-1 and examine the effects of its co-administration on food intake (FI) and body weight (BW) in mice. ***Methods:*** FI and c-Fos levels were measured in the feeding-centers of the brain in response to an intraperitoneal injection of saline, OXT, GLP-1 or OXT/GLP-1. The action potential frequency and cytosolic Ca^{2+} ($[Ca^{2+}]_i$) in response to OXT, GLP-1 or OXT/GLP-1were measured in *ex-vivo* PVN neuronal cultures. Finally, FI and BW changes were compared in diet induced obese mice treated with saline, OXT, GLP-1 or OXT/GLP-1 for 13 days. ***Results:*** Single injection of OXT/GLP-1 additively decreased FI, and increased c-Fos expression specifically in the paraventricular (PVN) and supraoptic nucleus (SON). 70% of GLP-1 receptor positive neurons in the PVN also expressed OXT receptors, and OXT/GLP-1 co-administration dramatically increased firing and $[Ca^{2+}]_i$ in the PVN OXT neurons. The chronic OXT/GLP-1 co-administration decreased BW without changing FI. ***Conclusion:*** Chronic OXT/GLP-1 co-administration decreases BW, possibly via the activation of PVN OXT neurons. OXT might be a promising candidate as an incretin co-agonist in obesity treatment.

Introduction

According to the World Health organization, worldwide obesity has nearly tripled within the past 50 years. In 2016, 1.9 billion adults were overweight, of these 650 million people were obese [1]. Obesity presents with a number of life-threatening co-morbidities such as diabetes, cardiac and inflammatory disease, and carries a severe mental health burden. [2, 3]. The prevention of obesity or the development of effective weight loss strategies for those already overweight are therefore critical.

Historically successful obesity drug development has been hampered by the serious adverse effects of these drugs. For example, 2,4-dinitrophenol (DNP), used for weight loss until the mid-twentieth century, caused hyperthermia, tachycardia, diaphoresis, tachypnea and could be fatal. [4, 5]. Rimonabant, a cannabinoid receptor antagonist, was recently withdraw from the European market, due to its' psychiatric impact, and potential to cause sever mood disorder(s) [5]. Sibutramine, which effects appetite, followed a similar pattern and was withdraw from the European, USA, Canadian market in 2002 [6].

The one exception to this rule is GLP-1 receptor agonists. Numerous studies demonstrated the successful use of the third generation GLP-1R agonist Semaglutide in weight loss and diabetes management [7, 8]. Injected Semaglutide mimics the systemic effects of glucagon-like-peptide (GLP-1) and, has been approved as the first line obesity drug by the U.S Food and Drug Administration (FDA) in mid-2021[5].

GLP-1 is peptide hormone secreted by intestinal enteroendocrine L cells, which stimulates pancreatic β–cell to secrete insulin [9]. It has been known that GLP-1 receptors (GLP-1R) are expressed in the cell bodies of nodose ganglion of vagal nerve and, peripheral GLP-1 reduce food intake via activation of vagal afferent neurons [10].

In addition to the intestine, endogenous GLP-1 peptide is produced in the brain. It has been shown that GLP-1 producing neurons are distributed in the nucleus of the solitary tract (NTS) of the brain stem [11, 12]. These GLP-1 neurons project to the hypothalamus, and impact on both feeding regulation and/or energy metabolism [11, 12]. GLP-1Rs are distributed throughout various brain regions specifically those which are important in the regulation of feeding and energy metabolism, such as paraventricular hypothalamic nucleus (PVN), arcuate nucleus (ARC), dorsomedial hypothalamic nucleus (DMH), nucleus tractus solitarius (NTS) and area postrema (AP) [13]. Perhaps not unsurprisingly, due to the effect of GLP-1R agonists on vagal nerve activity and gastric motility, nausea is the most frequent adverse effect reported by patients being treated with GLP-1R agonists [14]. In the Wegovy STEP trial, a quarter of participants experienced nausea and diarrhea [5]. In a bid to maximize weight loss while keeping the adverse effects of drugs to a minimum, a new class of drugs called gut hormone co-agonists, had been the focus of new developments in the fight against obesity [15].

Currently, several low dose co-agonists which target GLP-1, GIP and glucagon are in development, with the potential of synergistic metabolic benefits without the crippling side effects. Recently, a new GLP-1-glucose-dependent insulinotropic polypeptide (GIP) co-agonist, tirzepatide, was approved for treatment of type2 diabetes in 2022 by US FDA [15] and clinical trials for a triple GLP-1-GIP-glucagon agonist are ongoing [15].

The neuropeptide oxytocin (OXT) is a hormone secreted from hypothalamic OXT neurons, and is most well-known for its function in parturition and lactation [16]. However, work over the past 2 decades have shown OXT to be a pleiotropic hormone with wide implications for human health far beyond its reproductive functions [17]. It is

now well established that OXT plays a role in maternal behavior [18], pair bonding [19] and the perception of anxiety [20]. However, OXT also has a metabolic impact and it was demonstrated that OXT administration has an anti-obesity effect [21–23]. It has been known that OXT stimulate the neurons in the dorsal motor nucleus of the vagus (DMNV), which is the origin of the vagus nerve afferent pathway, and delays gastric emptying via vagal nerve activation to decreased food intake [24, 25]. Furthermore, OXT administration increase energy expenditure and reduce adipose tissue through enhanced lipolysis [21, 26] and chronic OXT treatment decrease BW in rodents [22] and primates [23]. In addition, it was shown that nasal treatment of OXT for 8 weeks decreased BW in humans [27]. Importantly, no significant adverse effects to OXT administration have been reported in human trials [28]. Interestingly, the anti-obesity effect of OXT is depended on the body mass index (BMI) and BW, i.e. OXT administration had little effect of lean mice or non-obese animals and humans [22, 29]. OXT receptors (OXTR) are distributed through the brain including the hypothalamus, brainstem [30] and nodose ganglion of the vagal nerve [31].

The aim of this study was therefore to evaluate OXT as a possible co-agonist for GLP-1 and the test the effects of GLP-1 and OXT co-administration on food intake and BW. The concept of the combination of an incretin hormone and a neuropeptide is highly novel, and this study contribute to expanding the potential of incretin-based treatments of obesity.

Materials and Methods

Animals

Ten to 12-week-old male C57BL/6J mice (purchased from Japan SLC (Japan)) were used for food intake measurement after intraperitoneal (IP) injection of GLP-1 and OXT, (BW: 22.1-29.2 g). The animals were maintained on a 12 hr light/dark cycle. (Turn on, 7:00; Turn off, 19:00), were housed in individual cages and fed a standard diet (CE-2: Clea, Osaka, Japan). All animals were habituated for at least 10 days before the experiment.

Six-week-old male C57BL/6J mice (purchased from Japan SLC (Shizuoka, Japan)) were used for chronic treatment with GLP-1 and OXT. These animals were fed a high fat diet (HFD32; Clea Osaka Japan) for 8 weeks. Thus, 14-week-old male mice were used for experiments.

Histological detection of OXT receptor (OXTR) positive neurons is technically demanding due to the lack of sensitive and specific antibodies for the OXTR [32]. Thus, 12-week-old male heterogeneous OXTR knock in mice $(oxtr)^{Venus\Delta Neo/+}$, in which part of the oxytocin receptor gene was replaced with Venus cDNA, were used for immunohistochemical analysis of OXTR expression [32]. These mice express the fluorescent Venus protein under the control of endogenous regulatory region of OXTR.

Experimental procedure and care of animals were carried out according to the Fukushima Medical University Institute of Animal Care and Use Committee (approval number 2023022, 2023021).

Food intake after IP injection of GLP-1 and OXT

On the day of experiment, food was removed at 16:00 (3 hrs before dark phase), and saline or GLP-1 (50 μg/kg/5ml, 100 μg/kg/5ml ; Human, 7-36 Amide, 4344-v, Peptide Institute, Osaka, Japan), or OXT (100 μg/kg/5ml , 200 μg/kg/5ml; 4084-v, Peptide Institute, Osaka, Japan) or both (GLP-1 100 and OXT 200 μg/kg/5ml) were IP injected at 19:00. The doses of GLP-1 and OXT were decided based on the previous reports [21, 33]. The animals were given food at 19:00 and food intake was then monitored for 24 hours.

c-Fos immunostaining after IP injection of GLP-1 and OXT

In order to identify the brain regions, which are related the anorexigenic effect of OXT and GLP-1, c-Fos expression after injection of the minimum effective dose of OXT plus GLP-1 were examined. Sixteen mice were divided into 4 groups: control, OXT, GLP-1 and OXT plus GLP-1(n = 4 in each group). On the day of experiment, food was removed at 9:00, and saline or GLP-1 (100 μg/kg/5ml), or OXT (200 μg/kg/5ml), or both (OXT 200 and GLP-1 100 μg/kg/5ml) were IP injected at 11:00. After 2h, animals were IP injected with a mixture of three types of anesthetic agents [composition; Medetomidine (0.003%, Domitor, Nippon Zenyaku Kogyo Co., Ltd., Koriyama, Japan), midazolam (0.04%, Dormicum, Astellas Pharma Inc., Tokyo, Japan), and butorphanol tartrate (0.05%, Vetorphale, Meiji Seika Pharma Co., Ltd., Tokyo, Japan)] (10 ml/kg) and perfused intracardially with 4% paraformaldehyde (PFA) and 0.2% picric acid. Serial coronal sections (40 μm thick) were collected from each mouse using a freezing microtome. The sections at 120 μm intervals between 0.50 mm and −7.92 mm from the bregma were used for immunostaining. Thus, around 60 sections from one mouse were used for immunostaining.

The sections were washed in PBS (0.01 M, pH7.4), then incubated for 20 min with 0.3% H_2O_2. Next, the sections were incubated for 1 h in a blocking solution comprising of 0.3% TritonX-100, 2% BSA, and 5% normal goat serum (NGS) and then incubated with rabbit anti-c-Fos antibody (1:2000; RPCA-c-Fos AP; Encor Biotechnology Inc. FLA) in the blocking solution overnight at 4 °C. Next, the sections were washed by PBS and incubated with biotinylated goat anti-rabbit IgG (diluted to 1:500, Vector Laboratories, CA) for 30 min, followed by incubation with an avidin-biotin-peroxidase complex (Vectastain Elite ABC Kit; Vector Laboratories, CA) for 60 min. Immunoreactions were visualized by incubation in a 0.02% diaminobenzidine solution containing 0.3% nickel ammonium and 0.015% H_2O_2 for 5 min. After color development, the sections were mounted on glass slides and covered. 4-5 (PVN), 4-5 (ARC), 3-4 (SON), 5-7(NTS), 3-4 (AP), and 5-7 (DMNV) sections were counted for c-Fos positive neurons under a light microscope. In order to avoid the variation of number of section made from each mouse, the numbers of c-Fos positive neuron was counted in each section and averaged by the number of sections.

For double immunostaining of c-Fos and OXT, c-Fos staining was performed similar as described above. c-Fos staining sections were incubated with mouse anti-oxytocin antibody (1:1000; MAB5296, Merck Millipore, MA) in the blocking solution overnight at 4 °C. Next, the sections were washed by PBS and incubated with biotinylated goat anti-rabbit IgG (diluted to 1:500, Vector Laboratories, CA) for 30 min, and were then incubated with an avidin-biotin-peroxidase complex (Vectastain Elite ABC Kit; Vector Laboratories, CA) for 60 min. Immunoreactions were visualized by incubation in a 0.02% diaminobenzidine solution containing 0.015% H_2O_2 for 5 min. After color development, the sections were mounted on glass slides and covered. In 4-5 (PVN) and 3-4 (SON)

sections, the numbers of c-Fos and OXT immune-positive neurons and double positive neurons were counted under a light microscope. Then, percentage of OXT positive neurons among the c-Fos positive neurons and percentage of c-Fos positive neurons among OXT positive neurons were calculated.

Immunostaining OXTR and GLP-1R

OXTR-Venus male mice were IP injected with a mixture of three types of anesthetic agents (10 ml/kg) and perfused intracardially with 4% paraformaldehyde (PFA) and 0.2% picric acid. Serial coronal sections (40 μm) were collected from each mouse using a freezing microtome. The PVN containing sections at 120 μm intervals between -0.58 mm and −1.22 mm from the bregma were used for immunostaining. Thus, 4-5 sections from one mouse were used for immunostaining. The sections were washed in PBS and incubated for 1 h in a blocking solution comprising of 0.1% TritonX-100, 2% BSA, and 5% normal goat serum (NGS).

For double immunostaining OXTR and OXT, sections were incubated with rabbit anti-GFP antibody (1:1000; A-11122, Thermo Fisher Scientific, MA) and with mouse anti-oxytocin antibody (1:1000; MAB5296, Merck Millipore, MA) in blocking solution overnight at 4 °C. Then sections were incubated with Alexa flour 488-labelled goat anti rabbit IgG (1:400, Life Technologies, CA) and, Alexa flour 594-labelled goat anti-mouse IgG (1:400; Life Technologies, CA) for 30 min.

For double immunostaining OXTR and GLP-1R, sections were incubated with chicken anti-GFP antibody (1:500; A11039, abcam, Cambridge, UK) and rabbit GLP-1R antibody (1:200, Thermo Fisher Scientific, MA) in blocking solution overnight at 4 °C. Then sections were incubated with Alexa flour 488-labelled goat anti chicken IgG (1:400, Life

Technologies, CA) and, Alexa flour 594-labelled goat anti-rabbit IgG (1:400; Life Technologies, CA, 1:400) for 30 min.

Sections were mounted on glass slides and covered. Confocal fluorescence images were acquired and OXTR positive neurons and OXT positive neurons and double positive neurons, or GLP-1R positive neurons and double positive neurons were counted.

Electrophysiology

OXTR-Venus male mice were IP injected with a mixture of three types of anesthetic agents (10 ml/kg) and brain was removed. Coronal brain slices (250 μm) containing the PVN were prepared. All electrophysiological experiments were performed as previously described [34]. Whole-cell recordings were made using an EPC 800 patch clamp amplifier (HEKA, Stuttgart, Germany) with filtering at 1 KHz using 4-5 MΩ electrodes. Coronal brain slices (250 μm) were prepared in an ice-cold solution containing (in mM) 230 sucrose, 2 KCl, 1 KH_2PO_4, 0.5 $CaCl_2$, 1 $MgCl_2$, 26 $NaHCO_3$, and 10 D-glucose. Oxytocin secretion from brain slices of the PVN has a rhythmic pattern with increased secretion in the early-light phase compared with the pre-dark phase [34] which would suggest a diurnal change of membrane potential in PVN OXT neurons. Thus, in order to avoid variation of membrane potential based on the diurnal change, all brain slices were prepared at around 10:00 am. The slices were recovered in artificial cerebral spinal fluid (aCSF), gassed with 95% O_2 and 5% CO_2, containing (in mM) 126 NaCl 2.5 KCl, 1.2 $MgCl_2$, 2.4 $CaCl_2$, 1.2 NaH_2PO_4, 21.4 $NaHCO_3$, and 10 D-glucose. Patch electrodes were filled with an internal solution containing (in mM) 120 K-gluconate, 10 KCl, 10 HEPES, 5 EGTA, 0.3 $CaCl_2$, 1 $MgCl_2$, 2 Mg-ATP, and 1 Na-GTP at pH 7.3 adjusted with KOH. The brain slices were then transferred to a recording chamber and continuously perfused

at 2–4 ml/min with aCSF gassed with 95% O_2 mad 5% CO_2. Whole-cell patch recordings were performed in a current clamp with a zero holding current. The membrane potentials of firing neurons were determined from slow time-scale recordings with a clear baseline. The concentrations of OXT (10^{-10} M) and GLP-1 (10^{-10} M) for patch clamp in brain slice were decided based on the concentration of OXT and GLP-1 used in single neurons, which are the minimum effective dose which induced Ca^{2+} release in this study. Data were analyzed using Clampfit software (Molecular devices, CA).

Preparation of single PVN neurons and measurement of $[Ca^{2+}]_i$ and subsequent immunocytochemistry in single neurons

Single neurons were prepared from the PVN according to previous reports [35] with slight modification. Briefly, untreated C57BL/6J mice were decapitated under anesthesia and brains were removed. Brain slices were prepared and the entire PVN were punched out. The tissues were incubated in a shaking water bath for 15 min at 36°C in Krebs-Ringer Bicarbonate Buffer (KRB) containing 20 units/ml papain (Sigma Chemical, St. Louis, MO), 1 mM cysteine, 0.015 mg/ml deoxyribonuclease, 0.75 mg/ml BSA, and 1 mM glucose. Following gentle trituration, the cell suspension was washed with KRB by centrifugation at 750 rpm for 5 min. The cells were re-suspended in KRB and distributed onto glass bottom dish. The cells were kept in a humidified chamber at 30 °C until measurements.

Cytosolic Ca^{2+} concentration ($[Ca^{2+}]_i$) was measured by ratiometric fura-2 microfluorometry combined with digital imaging, as previously reported [35]. Briefly, prepared single neurons on a glass-bottom dish were incubated with 2 mM fura-2/AM (Dojin chemical, Kumamoto, Japan) for 30 min at room temperature, placed in a chamber,

and superfused with KRB, containing GLP-1 (10^{-14}, 10^{-12} 10^{-10} M), OXT (10^{-14}, 10^{-12}, 10^{-10} M) or OXT/GLP-1 (combination of 10^{-12} M OXT and 10^{-12} M GLP-1) at 1 ml/min at 30°C. Cells loaded with fluorescent dye were illuminated by alternating 340 and 380 nm, and the resultant fluorescent images were captured. The ratio (F340/F380) images were produced by Aquacosmos version 2.6 (Hamamatsu Photonics, Hamamatsu, Japan).

After the $[Ca^{2+}]_i$ measurements, single neurons were fixed in 4% PFA overnight. For immunocytochemistry, staining was carried out as previously reported [35]. Briefly, cells were incubated for 10 min with PBS containing 3% H_2O_2. Then, sections were incubated in PBS containing 2% normal goat serum (Cat# 005-000-121; Jackson Laboratories Inc. PA) and 2% BSA (Cat# B2064, Sigma Aldrich, CA) and then incubated with rabbit anti-oxytocin polyclonal IgG (Cat# 20068; Immunostar Inc., WI; 1:2,000) overnight at 4 ºC. Subsequently, cells were washed in PBS and incubated with biotinylated goat anti-rabbit polyclonal IgG (Cat# BA-1000; Vector Laboratories Inc., CA; 1:500), and then with avidin-biotin complex (Cat# PK-6100; ABC kit; Vector Laboratories Inc., CA). Immunoreactions were visualized by incubation in a 0.02% diaminobenzidine solution containing 0.015% H_2O_2 for 5 min.

Calculation of $[Ca^{2+}]_i$ amplitude responses

Amplitudes of $[Ca^{2+}]_i$ responses to agents were calculated by subtracting the pre-stimulatory basal $[Ca^{2+}]_i$ ratio from the peak $[Ca^{2+}]_i$ ratio. Basal $[Ca^{2+}]_i$ ratio was defined as average of $[Ca^{2+}]_i$ for 3 min before stimulation. Peak $[Ca^{2+}]_i$ ratio was defined as peak value for 5 min or 10 min from the point of drug addition.

To combine individual $[Ca^{2+}]_i$ imaging with immunocytochemical data, at the end of $[Ca^{2+}]_i$ imaging, photographs of the cell in which $[Ca^{2+}]_i$ was recorded were taken.

Chronic OXT and GLP-1 treatment and measurement of plasma OXT

HFD-induced obese mice were divided 4 group. 1) saline group, 2) OXT group, 3) GLP-1 group and 4) OXT/GLP-1 group. These mice were anesthetized by a mixture of three types of anesthetic agents (10 ml/kg) and received surgical operation to implant osmotic mini-pumps (Alzet; model 2002 for 14days, CA) into subcutaneous at back side. Osmotic mini-pumps contained saline for the controls or OXT (400 μg/kg/day; 4084-v, Peptide Institute, Osaka, Japan) or GLP-1 (200 μg/kg/day; Human, 7-36 Amide, 4344-v, Peptide Institute, Osaka, Japan) or OXT/GLP-1(400 μg/kg/day, 200 μg/kg/day, respectively). The concentration of OXT and GLP-1 was calculated from individual BW, and each solution was filled into each osmotic minipump. Food and BW were measured every day at 17:00 (2 hours before the onset of the dark phase) for 13 days.

The dose of OXT and GLP-1 were decided based on the feeding experiment after IP injection of OXT and GLP-1 (Fig.1). The dose for chronic treatment of these peptides was twice the minimum effective dose, and the volume ratio of GLP-1 and OXT was 1:2. In order to examine the food efficacy to body weight gain [36], the amount of food intake / BW gain / day was calculated after 7 -13 days after diffusing each peptide.

At 14 days after chronic treatment of each agents, blood glucose was measured after 2 h fasting. Mice were anesthetized by a mixture of three types of anesthetic agents (10 ml/kg) and blood samples were collected in tubes containing EDTA and aprotinin. Plasma samples were collected between 11:00–13:00 under 2 h fasting conditions. Samples were centrifuged immediately at 4 °C at 3000 rpm for 15 min. The plasma samples were extracted by C18 Sep-Pak column (Waters, MA). Plasma OXT concentration was

measured by OXT EIA kit (Enzo Life Sciences/ Assay Designs, NY). Intra-assay and inter-assay variation of this kit were 12.6–13.3% and 11.8–20.9%, respectively.

Statistical analysis

All data are presented as mean ± SEM. The comparison of data from multiple groups was performed using a one-way ANOVA followed by Turkey's multiple range test. The comparison of data from multiple groups with time course was performed using repeated measures two-way ANOVA followed by Turkey's multiple range test. All statistical tests were two-tailed, with values of 0.05 considered statistically significant.

Results

OXT enhances anorexigenic effect of GLP-1

In order to identify the minimum effective dose of GLP-1 and OXT on food consumption, food intake was measured after IP injection of GLP-1 (50 μg/kg, 100 μg/kg) and OXT (100 μg/kg, 200 μg/kg) at 0.5 h, 1 h, 3 h, 6 h and 24 h time points. 50 μg/kg dose of GLP-1 had no effect on food intake at any time point, but 100 μg/kg dose GLP-1 decreased food intake at 3 h post injection by 22.1% ($F_{2, 120} = 5.99$, $P < 0.01$) [control 1.12 g ± 0.04 g vs GLP-1 100 ug/kg 0.88 ± 0.13 g] (Fig.1A). This data indicates that the minimum dose of GLP-1 to have an anorexigenic effect was 100 μg/kg in the present study. For OXT, a 200 μg/kg dose decreased food intake at 6 and 24 h after injection by 17.0% and 7.9% respectively ($F_{2, 102} = 7.204$, $P < 0.01$). [6 h control 1.85 ± 0.08 g, 6 h 200 μg/kg OXT 1.54 ± 0.07 g, 24 h control 4.28 ± 0.30 g, 24 h 200 g/kg OXT 3.9 ± 0.13 g] (Fig.1B).

Next, we examined the effect of OXT and GLP-1 co-administration. As shown Fig.1C, OXT co-administration significantly enhance the anorexigenic effects of GLP-1 at 3 h and 24 h after IP injection ($F_{3, 246} = 15.45$, $P < 0.01$). [3 h control 1.03 ± 0.07 g, 3 h OXT/GLP-1 0.68 ± 0.06 g, 24 h control 4.18 ± 0.17 g, 24 h OXT/GLP-1 3.30 ± 0.21 g]. Similar tendency has been detected at 2 h [control 0.7 ± 0.06 g, OXT/GLP-1 0.4 ± 0.05 g]. At 24 h, single OXT and GLP-1 injections decreased food intake by 10.1% ± 4.1 and 10.5% ± 4.5 compared with control, respectively. However, GLP-1 and OXT co-administration decreased food consumption by 20.9% ± 5.0. A clear additive effect of OXT and GLP-1 co-administration on food consumption was shown with an impact

visible from 3 h after co-administration. However, there were no significant differences in cumulative food intake in control and OXT/GLP-1 group at 36 h (Supplemental Fig. 1). Therefore, the anorexigenic effect mediated by IP injection of the OXT (200 μg/kg) plus GLP-1 (100 μg/kg) lasted for up to 24 h.

The distribution of c-Fos after injection of OXT/GLP-1

The appetite regulating circuits of the arcuate nucleus (ARC) and paraventricular nucleus (PVN) of the hypothalamus are divided into (1) the anorexigenic pro-opio melanocortin (POMC)/ cocaine and amphetamine related transcript (CART) neurons and (2) the orexigenic NAG neurons (neuropeptide Y (NPY), agouti-related protein (AGRP) and gamma-aminobutyric acid (GABA)ergic neurons) and are both GLP-1 targets. OXT, on the other hand, exerts its effect on appetite, food intake and metabolism through receptors expressed in the supraoptic nucleus (SON), with neurons projecting to the ARC and PVN [37].

Furthermore, the hypothalamus and brain stem are identified as key regions for feeding regulation and energy homeostasis [38]. The ARC in the hypothalamus and nucleus tractus solitarius (NTS) in the brain stem are key target for hormones vital to metabolic regulation, such as leptin and ghrelin as well as the incretins GLP-1 and GIP [38]. Anorexigenic POMC and orexigenic NAG neurons are distributed in the ARC and both GLP-1R and OXTR are expressed in these neurons [37, 39, 40]. Previous work showed that OXT positive neurons in the PVN and SON project to ARC, that PVN OXT positive neurons project to the brain stem, and OXT positive neurons are strongly associated with the regulation of feeding [41].

As OXT and GLP-1 co-administration had an anorexigenic effect, we therefore examined c-Fos expression levels post IP injection of the minimal effective dose of OXT and GLP-1. c-Fos gene expression is a general tool to indirectly visualize glutamatergic excitation in neurons as c-Fos expression is $[Ca^{2+}]_i$ sensitive [42, 43]. c-Fos expression was examined in the hypothalamus (PVN, ARC, SON) and brain stem (NTS, area postrema; AP, dorsal motor nucleus of the vagus; DMNV). There was no significant increase in c-Fos expression in ARC, NTS, AP and DMNV (Fig. 2A, C, E, F, G) following the administration of GLP-1 or OXT alone. However, OXT and GLP-1 co-administration induced enhanced c-Fos expression in both the PVN and SON (Fig.2B, D).

This experiment for detecting c-Fos was performed during the light phase, but the feeding experiments (Fig. 1) were performed during the dark phase. In order to examine the influence of injection timing (light and dark phase), c-Fos expression in these brain regions after OXT/GLP-1 injection in the light or dark phase were examined (Supplemental Fig. 2). As shown in Supplemental Fig. 2, there were no differences in c-Fos expression after OXT/GLP-1 injection during the light or dark phase. This data indicates that the injection of OXT/GLP-1 during the light or dark phase similarly activate the neurons in these brain regions.

Therefore, the data in Fig.2 would indicate that the additive effect of OXT on GLP-1 on appetite is mediated via circuits of the hypothalamus.

Previous reports have shown that IP OXT administration can activate PVN OXT positive neurons [44, 45]. In order to identify the neuronal population activated by OXT and GLP-1 co-administration, we performed double staining of c-Fos and OXT in the PVN (Fig.3A-D) and SON.

In order to clarify how many of the neurons activated by co-administration of OXT and GLP-1 express OXT endogenously, the percentage of OXT positive neurons which overlap with c-Fos positive neurons were analyzed. In the PVN, the percentage of OXT positive neurons which overlap with c-Fos positive neurons were 7.3 ± 1.6%, 17.4 ± 1.3%, 14.1 ± 1.5% and 16.0 ± 0.6% in control, OXT, GLP-1 and co-administration of OXT and GLP-1 group, respectively (Fig.3E). The percentage of activated OXT positive neurons in the PVN for the OXT treated, GLP-1 treated and co-administration of OXT and GLP-1 group were therefore significantly increased compared with control for all three treatments and no additive effect was observed ($F_{3, 12} = 11.99$, $P < 0.01$). Interestingly, there were no significant different among these three treated groups (Fig. 3E). In the SON, the percentage of activated OXT neurons were 6.4 ± 2.5%, 14.4 ± 5.7%, 25.6 ± 5.0% and 24.3 ± 1.1% in control, OXT, GLP-1 and co-administration of OXT and GLP-1 group, respectively (Fig.3F). The percentage of activated OXT neurons in the SON for the GLP-1 treated and co-administration of OXT and GLP-1 group were significantly increased compared with control ($F_{3, 12} = 5.1$, $P < 0.05$).

In order to establish the reverse relationship – how many of OXT positive neurons are activated by OXT and GLP-1 treatment, the total percentage of c-Fos positive neurons which overlaps with OXT positive neurons were calculated. The percentage of c-Fos positive neurons which overlaps with OXT expressing neurons in the PVN were 5.2 ± 0.8%, 21.4 ± 3.2%, 20.2 ± 4.7% and 20.2 ± 1.8% in control, OXT treated, GLP-1 treated and co-administration of OXT and GLP-1 group, respectively (Fig. 3G). As seen in Fig 3A-D the percentage of c-Fos positive neurons overlapping with OXT expressing neurons in OXT treated, GLP-1 treated and co-administration of OXT and GLP-1 group was significantly increased compared with control for all three treatments and no additive

effect was observed ($F_{3, 12} = 6.16$, $P < 0.01$). The percentage of c-Fos positive neurons in OXT expressing neurons in the SON were 7.0 ± 3.8%, 13.5 ± 4.8%, 28.9 ± 7.6% and 25.9 ± 1.3% in control, OXT treated, GLP-1 treated and co-administration of OXT and GLP-1 group, respectively (Fig. 3H). The percentage of c-Fos positive OXT neurons were significantly increased for the GLP-1 group.

Overall, treatment with OXT, GLP-1 or co-administration showed increased activation of OXT positive neurons in regions of the brain associated with appetite and energy metabolism.

Co-localization of OXT receptor and GLP-1 receptors in PVN

In order to establish the expression of OXTR and GLP-1R in the PVN, we performed double staining of OXTR and GLP-1R in the PVN. OXTR were distributed throughout the PVN (Fig.4 Ai). On the other hand, GLP-1Rs were distributed in the medial area of PVN (Fig.4 Aii) with a large portion of GLP-1 receptor expressing cells co-localizing with OXTR positive cells (Fig. 4Aiii). 68.6 ± 5.1% of GLP-1R positive cells were OXTR positive (Fig. 4B). Interestingly, 53.1 ± 4% of OXT positive neurons expressed OXTRs (Fig. 4C, D).

This data indicates that the majority of OXTR positive neurons are expressing GLP-1Rs and these neuronal populations is likely to be the target of GLP-1 and OXT co-administration.

Electrophysiological analysis of additive effect of OXT and GLP-1 in OXTR neurons

The previous experiment showed that the majority of GLP-1R positive neurons also express OXTR in the PVN. Thus, OXTR positive neurons might be a target of co-

administration of GLP-1 and OXT (Fig.4 A, B). In order to examine the additive effect of OXT and GLP-1 administration on the activity of PVN neurons, electrical activities of OXTR positive neurons were recorded after the addition of OXT, GLP-1 and co-administration of OXT and GLP-1 using brain slice patch clamp recordings from $(oxtr)^{Venus\Delta Neo/+}$ (OXTR-Venus) mice [32].

When comparing the electrical activities of neurons following the application of OXT (Fig. 5A), GLP-1 (Fig.5B) or both (Fig. 5C), single application of OXT or GLP-1 significantly increased the membrane potential compared to control (increase of membrane potential being 2.13 ± 1.1 mV for OXT and 5.5 ± 2.17 mV for GLP-1) (Fig. 5D), but failed to induce a significant increase in action potential firing (Fig. 5E). However, co-administration of OXT and GLP-1 significantly increased membrane potential (Fig. 5D) and strongly induced action potential firing (Fig. 5E) (increase of membrane potential being 10.39 ± 2.48 mV (Fig. 5E) and firing frequency of action potential firing for applying both OXT and GLP-1 was 4.89 ± 2.37 Hz compared to control: 0.03 ± 0.03, OXT: 0.15 ± 0.1, GLP-1: 0.16 ± 0.13 (Fig. 5E)). These results clearly indicate that single OXT and single GLP-1 administration does increase the membrane potential. However, co-administration of OXT and GLP-1 increased action potential firing frequency via increasing membrane potential to over threshold.

The effect of OXT and GLP-1 on cytosolic Ca^{2+} $[Ca^{2+}]_i$ changes in single OXT positive neurons

Next, we examined the effects of exogenous OXT and GLP-1 addition to *ex vivo* cultured, single OXT positive neurons isolated from the PVN using Ca^{2+}imaging. In order to establish the minimum effective dose which will increase $[Ca^{2+}]_i$ in single OXT

positive neurons 10^{-14}, 10^{-12} and 10^{-10} M OXT and GLP-1 were applied to single, isolated PVN neurons, respectively.

Administration of 10^{-14} and 10^{-12} M GLP-1 or OXT had no effect of $[Ca^{2+}]_i$ in single PVN neurons (Fig. 6A, B, E, F). However, both 10^{-10} M OXT and 10^{-10} M GLP-1 increased $[Ca^{2+}]_i$ as measured by fula-2 fluorescence in single PVN neurons (Fig. 6C, G). The amplitude of $[Ca^{2+}]_i$ in 10^{-10} M OXT and GLP-1 were significantly increased compared with control KRB (0) (Fig.6 D, H). The percentage of OXT positive neurons in this *ex vivo* single PVN neuronal culture were 49.5% (90 OXT positive neurons within 182 analyzed neurons). This data indicate that 10^{-12} M OXT or GLP-1 did not increase $[Ca^{2+}]_i$ in *ex vivo* PVN neurons when administered on their own.

Next, the effects of exogenous OXT and GLP-1 co-administration to single OXT positive neurons isolated from the PVN were examined. As expected, there were no response to 10^{-12} M OXT and 10^{-12} M GLP-1 in the single OXT neuron (Fig. 6I). However, co-administration of 10^{-12} M OXT and 10^{-12} M GLP-1 increased $[Ca^{2+}]_i$ in single OXT neurons. The amplitude of $[Ca^{2+}]_i$ during co-administration of OXT and GLP-1 was significantly increased compared with control ($F_{4,\ 45} = 6.9$, $P < 0.01$) (Fig. 6J). Surprisingly, this $[Ca^{2+}]_i$ increase was continuous and cumulative even after co-administration was withdrawn, and continued until the recording was terminated at 75 min (Fig.6 I, J). When comparing the area under the curve (AUC) within 5 min and 5-10 min after beginning of dual administration of OXT and GLP-1, next 5 min of AUC of $[Ca^{2+}]_i$ was significantly increased compared with first 5 min of AUC of $[Ca^{2+}]_i$.

This result indicates that co-administration of OXT and GLP-1 has a strong additive and continuous activatory effect on OXT positive neurons.

Sub chronic effect of OXT and GLP-1 on food intake and BW in high fat diet induced obese mice.

In order to examine the additive effect of OXT and GLP-1 on BW, OXT and GLP-1 were co-delivered by osmotic minipump for 13 days. The BW after eight weeks-HFD feeding were 46.3 ± 0.7g in control group, 47.5 ± 0.6 g for OXT group, 47.3 ± 0.9 g for GLP-1 group and 48.7 ± 2.2 g for OXT/GLP-1 group, and there were no significant different in BW among these groups ($F_{3, 15} = 0.5$, $P > 0.05$). The dose of OXT and GLP-1 were 400 μg/kg/day and 200 μg/kg/day, respectively. These doses correspond to the two times of minimum anorexigenic effect dose (Fig. 1C). As expected, both low level administration of OXT and GLP-1 had a tendency towards decreased BW, but there was no statistically significant difference in the OXT group and GLP-1 group when compared to control, respectively (Fig.7A). However, BW change in OXT/GLP-1 treatment group significantly decreased compared to control from days 3 to 13 after pump surgery ($F_{3, 210} = 36.59$, $P < 0.01$) (Fig.7A). The percentage of BW change from initial BW were 5.0 ± 1.2%, 0.3 ± 0.7%, 1.5 ± 0.9% and -3.9 ± 2.7% in control, OXT group, GLP-1 group and OXT/GLP-1 group, respectively (Fig.7D). The total % of BW change in OXT/GLP-1 group was significantly decreased when compared with control ($F_{3, 15} = 4.6$, $P < 0.05$) (Fig.7D). Interestingly, the daily food intake in GLP-1 group at day 1 was significantly decreased when compared with control ($F_{3, 195} = 3.31$, $P < 0.05$) (Fig. 7B). However, there were no significant differences in total amount of food intake for 13 days (Fig.7E) and blood glucose levels among the 4 groups (Fig.7F). In order to examine the food efficacy to body weight gain, food efficacy was calculated after 7 -13 days following the start of peptide diffusion, when mice were considered to be fully recovered from pump implanting surgery. Food efficacies were significantly decreased in OXT/GLP-1 group

compared with control group ($F_{3, 105} = 23.2$, $P < 0.01$) (Fig.7C). At day 13, food efficacy in OXT/GLP-1 group was significantly decreased compared with other groups (Control; 0.65 ± 0.15, OXT; 0.04 ± 0.10, GLP-1; 0.20 ± 0.11, OXT/GLP-1; -0.81 ± 0.57) (Fig.7C). This data suggests increased energy expenditure in the OXT/GLP-1 treated group.

The plasma OXT levels in OXT and OXT/GLP-1 administered groups were similarly significantly increased compared with the control and GLP-1 group, respectively ($F_{3, 17} = 23.55$, $P < 0.01$) (Fig.7G).

On the other hand, sub chronic treatment of OXT and GLP-1in lean mice had no effect on BW gain, food intake, food efficacy, % of BW change, total food intake and fasting blood glucose (Supplemental Fig. 3).

The data presented here collectively indicate that chronic low dose administration of OXT and GLP-1 decrease BW without effecting food intake in obese mice.

Next, in order to rule out any possible negative effects of sub-chronic treatment of OXT and GLP-1 on endogenously expressing OXT neurons, the number of OXT neurons, intensity of OXT expression, and number of caspase-3 positive neurons (apoptosis marker) [46] were examined by immunohistochemistry after sub chronic treatment of OXT and GLP-1 (Supplemental Fig. 4). OXT/GLP-1 treatment for 13 days had no effect on the number of OXT neurons (Supplemental Fig. 4A, B), the number of caspase-3 positive neurons (Supplemental Fig. 4A, C), and percentage of caspase-3 positive neurons in OXT neurons (Supplemental Fig 4A, D) in the PVN. However, OXT/GLP-1 treatment for 13 days significantly increased OXT specific fluorescence (Supplemental Fig.4A, E). This data would suggest that low dose OXT/GLP-1 treatment had no detrimental effects on OXT neurons, and apoptosis pathways remained unaltered.

Discussion

Here we report for the first time the positive systemic effects of low-dose, subcutaneous co-administration of OXT and GLP-1 on diet-induced obese mice. Interestingly, Lee et al. [47] reported that the sub-chronic co-administration to the third ventricle by the injection of OXT and GLP-1 canceled out the reduction in body weight and food intake in diet-induced obese mice which were shown to be promoted by the administration of either one of the peptides alone. This study therefore suggests that the central co-administration of OXT and GLP-1 negates the metabolic benefits of either one of the peptides administered alone [47]. This report differs from the results we show here for the systemic injection of OXT and GLP-1. It is well established that both the dose and route of OXT administration impacts on the metabolic impact of this drug in mammals [48]. In Lee et al., centrally injected [OXT] and [GLP-1] were 1.28 nmol/day and 16.01nmol/day, respectively (mol:mol ratio; OXT:GLP-1 = 1:12) in obese mice. For the study reported here, the dosage of subcutaneously injected OXT and GLP-1 were 400 nmol/kg and 60.5 nmol/kg, respectively (mol:mol ratio; OXT:GLP-1 = 6.6:1); as was experimentally established ratio based on the lowest effective dose for each peptide (Fig. 1). Thus, in our study reported here, the ratio of OXT to GLP-1 is the opposite (more OXT than GLP-1) and higher [OXT] were used when compared to the peptide levels used in Lee et al [47]. Our present results therefore suggest that the administration route, dose and ratio of OXT to GLP-1 may all impact on the metabolic benefit driven by OXT mediated signaling pathways in obese mammals.

A comprehensive systematic review of the effects of various doses of OXT on feeding in mammals showed that a single dose of intracerebroventricular, intraperitoneal,

subcutaneous and intravenous injection of OXT were all found to reduce feeding in mammals [48]. Although anorexigenic effects of chronic (both central and peripheral administration) OXT persist to the end of the third week in rodent studies, this anorexigenic effect was not significant in the meta-analysis testing the effects of chronic administration [48]. Our current data, which showed that a single dose of OXT and GLP-1decreased food intake, but chronic co-administration of OXT and GLP-1 has no effect on the food intake, is therefore in agreement with data shown for previous studies where only OXT was administered [48]. This work highlights the many challenges of working with OXT, where the dose, weight of the animal, administration route and duration of treatment can all have an impact on the outcome.

There are numerous reports that shows endogenous or exogenous OXT is associated with the control of food intake and BW regulation. Fasting result in reduced OXT expression in the hypothalamus [49], and refeeding after fasting activate OXT neurons in hypothalamus [50]. In addition, obesity decreases serum OXT levels in rodents and human [51–53], and serum OXT levels negatively correlates with BMI in humans [52, 53].

Peripheral and intracerebroventricular (ICV) injection of OXT decreased food intake [21, 40], and increased energy expenditure [21, 51]. On the other hand, pharmacological blockage or genetic knockdown of OXTR increased food intake [54, 55], suggesting that endogenous OXT is involved in homeostatic feeding. However, OXTR-and OXT-deficient mice developed obesity, despite food intake and locomotor activity remaining unchanged [56, 57], strongly suggesting that a lack of OXT and OXTR mediated signalling reduce energy expenditure [58].

Furthermore, OXT-deficient mice do have an enhanced sweet preference [59]. Therefore, OXT-OXTR systems plays an important role in reward related feeding, as well as regulating homeostatic feeding, energy expenditure and BW.

On the other hand, the physiological importance of endogenous GLP-1 in feeding behaviour and homeostasis is well understood [60]. GLP-1R blockade in CNS increases food intake [61] and chronic central antagonism of the GLP-1R for one week produced hyperphagia and weight gain in high-fat diet–fed obese mice [62]. GLP-1 and its analogues reduce food intake and BW in both experimental animal models for obesity and humans [63, 64]. To our knowledge, we are the first to report the effect of OXT and GLP-1 co-administration on the feeding regulatory centres of the brain.

It is known that the neurons in NTS of brain stem and ARC of hypothalamus are central to the regulation of feeding and metabolism and are under both vagal nerve and endocrine control, and the neurons in the NTS and ARC are referred as first order neurons in feeding control circuits of the mammalian brain [65].

The NTS is the primary site for innervation by the vagal afferents from the gut [66]. Both of OXTR and GLP-1R are distributed in the nodose ganglion of the vagal afferent [11,31]. Thus, is likely that peripheral administration of OXT and GLP-1 could stimulate the vagal afferent. However, our results show that following a single injection of OXT and GLP-1, that c-Fos positive neurons increased in both the PVN and SON, but not in the NTS and ARC. It is therefore likely that this additive anorexigenic effect is mediated by PVN and SON neurons at this dose (OXT: 100 μg/kg, GLP-1: 200 μg/kg).

Furthermore, there were no additive effect on the number of c-Fos expression in the brain stem (NTS, AP and DMNV, Fig. 2E-G). As shown in Fig. 2E, the number of c-Fos

expressing neurons in the OXT/GLP-1 treated group is very similar to that of the OXT treated group. On the other hand, the number of c-Fos expressing neurons in GLP-1 treated group are very similar to that of the control. These results suggest that c-Fos expression in the OXT/GLP-1 treated group reflects the effect of OXT. Thus, a possible explanation is that only 200 μg/kg OXT is capable to stimulate neurons in the nodose ganglion, but not 100 μg/kg GLP-1. However, there were no significant differences in the number of c-Fos expressing neurons between the control and OXT group and the OXT/GLP-1 group, respectively. This would suggest that there was relatively little activation of the vagal afferent even under co-treatment of 200 μg/kg OXT and 100 μg/kg GLP-1. The anorexigenic effect mediated by vagal afferent strongly affect gastric motility via the vago-vagal reflex, which induce nausea, vomiting, as adverse effect of the anorexigenic effect [67]. Therefore, drugs which has an anorexigenic effect while avoiding activation from the vagal nerve will be less likely to cause nausea and could be a real advantage as an obesity drug. As a caveat, since we examined only one dose of OXT (200 μg/kg) and GLP-1 (100 μg/kg), we cannot completely exclude the involvement of the vagal afferent in OXT-GLP-1 mediated signaling cascades.

The ARC is one of the most important brain areas to regulate food intake and energy homeostasis [65]. The ARC is the origin of the first order neurons (NAG and POMC neurons) which project to second order neurons in the PVN, and regulate food intake behavior [38]. However, our work showed no additive effect on c-Fos expression in the ARC in response to a single dose of IP co-administered 200 μg/kg OXT and 100 μg/kg GLP-1 (Fig.2C). Similar with NTS, as we examined only one dose of OXT (200 μg/kg)

and GLP-1 (100 μg/kg), we cannot completely exclude the involvement of the ARC in the OXT-GLP-1 mediated effects we report here.

How do OXT and GLP-1 affect the neurons in PVN and SON? The low dose OXT and GLP-1 used in this study will most likely cross the blood brain barrier (BBB) into the parenchyma. It has been reported that both OXT and GLP-1 can cross the BBB and reaches the brain parenchyma [68–70]. Our study showed that approximately, 70% of GLP-1R positive neurons express OXTR (Fig. 4A, B) in the PVN. Thus, it is feasible that the co-administered OXT and GLP-1 impact identical neurons which express both OXTR and GLP-1R, simultaneously, and increased c-Fos expression, via dual activation of OXTR and GLP-1R.

This idea is corroborated by the slice patch clamp data which show a clear additive effect of OXT and GLP-1 on the action potential in the PVN neurons (Fig.5). As shown Fig,5D, 10^{-10} M OXT and 10^{-10} M GLP-1 significantly increased membrane potential compared with control, but not increased firing frequency (Fig. 5E), respectively. However, co-administration significantly increased both membrane potential and firing frequency, compared with control (Fig. 5D, E). These data suggested the activation of both OXTR and GLP-1R increased firing frequency of action potential via increasing membrane potential to over threshold in the PVN neurons.

Supporting the slice patch clamp data, co-administration of 10^{-12} M OXT and GLP-1, which dose alone did not induce $[Ca^{2+}]_i$ increase in PVN neurons, significantly increased $[Ca^{2+}]_i$ in PVN OXT neurons (Fig. 6I). Surprisingly, this increase was continuous, even after treatment was washed out (Fig. 6I-K). The robust increase in $[Ca^{2+}]_i$ are most likely mediated by both Gq and Gs signaling as G protein-coupled receptor (GPR) 40 and

GPR119 is known to signal through Gq and Gs, respectively [71]. Gq signalling evoke Ca^{2+} release via the IP3R in endoplasmic reticulum. On the other hand, Gs signal evoke Ca^{2+} spikes via L-type voltage-dependent Ca^{2+} channel (LVDCC) and ryanodine receptor in the endoplasmic reticulum. It has been reported that Gq and Gs signaling in enteroendocrine cells act in synergy to increase $[Ca^{2+}]_i$ and regulate GLP-1 secretion [71].

The GLP-1R is well known to couple with Gs family members [72, 73]. On the other hand, Gq coupled OXTRs are expressed in the brain, and a wide range of signal transduction pathways could potentially be regulated by OXTR activation in the adult brain [74]. Similar to GPR40 and GPR119, dual activation of GLP-1R and OXTR may synergistically amplify the cellular signaling events and evoke continuous $[Ca^{2+}]_i$ increase.

Intracellular calcium links synaptic activity to c-fos gene expression during enhanced neuronal activity [43]. This synergistic effect for $[Ca^{2+}]_i$ increase by OXT and GLP-1 are in agreement with the data of c-Fos expression in the PVN after IP co-administration of OXT and GLP-1 (Fig. 2). It is therefore possible that the neurons which were not responsive to either low dose OXT alone or low dose GLP-1 alone were activated when both peptides were added. Therefore, the data suggest that peripheral low dose co-administration of OXT and GLP-1 can induce neuronal activation in specific brain regions, via synergistic signal amplification through OXTR and GLP-1R.

Extrapolating from the effect of acute co-administration of OXT and GLP-1 on the PVN, chronic minipump administration of these peptides should result in a chronic activation of the PVN and should induce a reduction in BW. This was indeed the case and dual treated mice showed a significant weight loss compared to control saline in HFD induced

obese mice (Fig7), but not in SD fed lean mice (Supplemental Fig. 3). Considering the weight changes relative to the amount of food intake (Fig. 7C), it is most likely that energy expenditure was increased in dual treated obese mice.

Previous work forms our laboratory showed that ablation of PVN to DVC neural circuitry using the tetracycline (tet)-off system, increased BW gain with aging, with no effect on food intake [36]. Specific ablation of PVN OXT neurons in HFD induced mice increased BW, reduced energy expenditure, without changing food intake [75], and ablation of PVN OXT neurons has no effect on food intake, but cause a significant decrease in rectal temperature and brown adipose tissue in response to cold exposure stress [76]. Therefore, from these reports and our current data of food efficacy, chronic activation of PVN OXT may play an important role in the regulation of energy expenditure, rather than food intake. This suggestion is in line with the meta-analysis by Leslie et al. [48], which analyzed the effect of OXT on food intake. PVN OXT neurons may therefore play an important role in maintaining energy homeostasis when animals are exposed to physiological stress (e.g. aging, high calorie food, cold exposure).

As a clinical implication, the discovery of gut hormone co-agonists, for the treatment of obesity has been is an exciting new area of research [15]. Our current study explores the usefulness of a gut hormone-neuropeptide co-agonist for the treatment of obesity, with the potential to circumvent the nausea-inducing activation of the vagal nerve. In the Wegovy STEP trial, a quarter of participants experienced nausea and diarrhea, and furthermore long-term use of anti-obesity drugs places a heavy financial burden on patients [5]. As the low dose co-administration of OXT and GLP-1 reduced BW in diet-induced obese mice, while having little effect on NTS activation, and by extrapolation

the vagal nerve, it is possible that this drug combination will have fewer adverse effects, such as nausea and vomiting.

However, our current research has limitations. First, this work examined the effect of OXT/GLP-1 only in male mice. Second, this work examined only one dose of OXT/GLP-1 (combination of 200 μg/kg and 100 μg/kg, respectively in acute effects; combination of 400 μg/kg and 200 μg/kg, respectively in sub-chronic effects). In-depth future studies to ascertain the effects of sex, administration route, dose and side effects remain necessary.

In summary, our study showed that the single acute co-administration of OXT and GLP-1 decreased food intake additively in lean mice and that the, chronic co-administration of OXT and GLP-1 to HFD diet-induced obese mice decreased BW gain additively, with no effect on food intake. It is most likely that this decline of food intake in lean mice and inhibition of BW gain in obese mice by co-administration of OXT and GLP-1 were mediated by the activation of OXT positive neurons in the PVN.

Acknowledgement

The authors thank Ms. Rie Ohashi of Fukushima Medical University for her technical support.

Statement of Ethics

This study protocol was reviewed and approved by Fukushima Medical University Institute of Animal Care and Use Committee, approval number 2023022, 2023021.

Conflict of Interest Statement

The authors have no conflicts of interest to declare.

Funding Sources

This work was supported by JSPS KAKENHI Grant Numbers JP22K11755, JP18K08483 for YM, and JP20K08865, JP23K08012 for KS.

Author Contributions

Y. M, H.d.W and K.S conceived and designed the project. Y.M, S.Y. and K.S performed experiments and analyzed data; Y. M, H.d.W., K.S. prepared figures, edited and revised the manuscript, and drafted manuscript; Y. M, H.d.W., K.S. interpreted results of experiment; K.N and S.H. provided OXTR-Venus mice.

Data Availability Statement

Additional details regarding data and protocols that support the finding of this study are available from the corresponding author upon request.

Reference

[1] World health organization. Obesity and overweight. [cited 2023 Nov. 13]. Available from: https://www.who.int/news-room/fact-sheets/detail/obesity-and-overweight

[2] Valenzuela PL, Carrera-Bastos P, Castillo-García A, Lieberman DE, Santos-Lozano A. Obesity and the risk of cardiometabolic diseases. Nat Rev Cardiol. 2023;20(7):475-494. DOI: 10.1038/s41569-023-00847-5

[3] Plackett B. The vicious cycle of depression and obesity. Nature. 2022;608(7924):S42-S43. DOI: 10.1038/d41586-022-02207-8.

[4] Grundlingh J, Dargan PI, El-Zanfaly M, Wood DM. 2,4-dinitrophenol (DNP): a weight loss agent with significant acute toxicity and risk of death. J Med Toxicol. 2011;7(3):205-12. DOI: 10.1007/s13181-011-0162-6.

[5] Senior M. After GLP-1, what's next for weight loss? Nat Biotechnol. 2023;41(6):740-743. DOI: 10.1038/s41587-023-01818-4.

[6] Onakpoya IJ, Heneghan CJ, Aronson JK. Post-marketing withdrawal of anti-obesity medicinal products because of adverse drug reactions: a systematic review. BMC Med. 2016;14(1):191. DOI: 10.1186/s12916-016-0735-y.

[7] Wilding JPH, Batterham RL, Calanna S, Davies M, Van Gaal LF, Lingvay I, et al. STEP 1 Study Group. Once-Weekly Semaglutide in adults with overweight or obesity. N Engl J Med. 2021;384(11):989-1002. DOI: 10.1056/NEJMoa2032183.

[8] Gribble FM, O'Rahilly S. Obesity therapeutics: The end of the beginning. Cell Metab. 2021;33(4):705-706. DOI: 10.1016/j.cmet.2021.03.012.

[9] Drucker DJ, Brubaker PL. Proglucagon gene expression is regulated by a cyclic AMP-dependent pathway in rat intestine. Proc Natl Acad Sci U S A. 1989;86(11):3953-7. DOI: 10.1073/pnas.86.11.3953.

[10] Barrera JG, Sandoval DA, D'Alessio DA, Seeley RJ. GLP-1 and energy balance: an integrated model of short-term and long-term control. Nat Rev Endocrinol. 2011;7(9):507-16. DOI: 10.1038/nrendo.2011.77.

[11] Brierley DI, Holt MK, Singh A, de Araujo A, McDougle M, Vergara M, et al. Central and peripheral GLP-1 systems independently suppress eating. Nat Metab. 2021;3(2):258-273. DOI: 10.1038/s42255-021-00344-4.

[12] Maejima Y, Yokota S, Shimizu M, Horita S, Kobayashi D, Hazama A, et al. The deletion of glucagon-like peptide-1 receptors expressing neurons in the dorsomedial hypothalamic nucleus disrupts the diurnal feeding pattern and induces hyperphagia and obesity. Nutr Metab (Lond). 2021;18(1):58. DOI: 10.1186/s12986-021-00582-z.

[13] Cork SC, Richards JE, Holt MK, Gribble FM, Reimann F, Trapp S. Distribution and characterisation of Glucagon-like peptide-1 receptor expressing cells in the mouse brain. Mol Metab. 2015;4(10):718-31. DOI: 10.1016/j.molmet.2015.07.008.

[14] Meier JJ. GLP-1 receptor agonists for individualized treatment of type 2 diabetes mellitus. Nat Rev Endocrinol. 2012;8(12):728-42. DOI: 10.1038/nrendo.2012.140.

[15] Nogueiras R, Nauck MA, Tschöp MH. Gut hormone co-agonists for the treatment of obesity: from bench to bedside. Nat Metab. 2023;5(6):933-944. DOI: 10.1038/s42255-023-00812-z.

[16] Dale HH. On some physiological actions of ergot. J Physiol. 1906;34(3):163-206. DOI: 10.1113/jphysiol.1906.sp001148.

[17] Carter CS, Kenkel WM, MacLean EL, Wilson SR, Perkeybile AM, Yee JR, et al. Is Oxytocin "Nature's Medicine"? Pharmacol Rev. 2020;72(4):829-861. DOI: 10.1124/pr.120.019398.

[18] Jin D, Liu HX, Hirai H, Torashima T, Nagai T, Lopatina O, et al. CD38 is critical for social behaviour by regulating oxytocin secretion. Nature. 2007;446(7131):41-5. DOI: 10.1038/nature05526.

[19] Walum H, Young LJ. The neural mechanisms and circuitry of the pair bond. Nat Rev Neurosci. 2018;19(11):643-654. DOI: 10.1038/s41583-018-0072-6.

[20] McCall C, Singer T. The animal and human neuroendocrinology of social cognition, motivation and behavior. Nat Neurosci. 2012;15(5):681-8. DOI: 10.1038/nn.3084.

[21] Maejima Y, Iwasaki Y, Yamahara Y, Kodaira M, Sedbazar U, Yada T. Peripheral oxytocin treatment ameliorates obesity by reducing food intake and visceral fat mass. Aging (Albany NY). 2011;3(12):1169-77. DOI: 10.18632/aging.100408.

[22] Maejima Y, Aoyama M, Sakamoto K, Jojima T, Aso Y, Takasu K, et al. Impact of sex, fat distribution and initial body weight on oxytocin's body weight regulation. Sci Rep. 2017;7(1):8599. DOI: 10.1038/s41598-017-09318-7.

[23] Blevins JE, Graham JL, Morton GJ, Bales KL, Schwartz MW, Baskin DG, et al. Chronic oxytocin administration inhibits food intake, increases energy expenditure, and produces weight loss in fructose-fed obese rhesus monkeys. Am J Physiol Regul Integr Comp Physiol. 2015;308(5):R431-8. DOI: 10.1152/ajpregu.00441.2014.

[24] Travagli RA, Anselmi L. Vagal neurocircuitry and its influence on gastric motility. Nat Rev Gastroenterol Hepatol. 2016;13(7):389-401. DOI: 10.1038/nrgastro.2016.76.

[25] Jiang Y, Travagli RA. Hypothalamic-vagal oxytocinergic neurocircuitry modulates gastric emptying and motility following stress. J Physiol. 2020 Nov;598(21):4941-4955. DOI: 10.1113/JP280023.

[26] Deblon N, Veyrat-Durebex C, Bourgoin L, Caillon A, Bussier AL, Petrosino S, et al. Mechanisms of the anti-obesity effects of oxytocin in diet-induced obese rats. PLoS One. 2011;6(9):e25565. DOI: 10.1371/journal.pone.0025565.

[27] Zhang H, Wu C, Chen Q, Chen X, Xu Z, Wu J, et al. Treatment of obesity and diabetes using oxytocin or analogs in patients and mouse models. PLoS One. 2013;8(5):e61477. DOI: 10.1371/journal.pone.0061477.

[28] Lawson EA, Marengi DA, DeSanti RL, Holmes TM, Schoenfeld DA, Tolley CJ. Oxytocin reduces caloric intake in men. Obesity (Silver Spring). 2015;23(5):950-6. DOI: 10.1002/oby.21069.

[29] Thienel M, Fritsche A, Heinrichs M, Peter A, Ewers M, Lehnert H, et al. Oxytocin's inhibitory effect on food intake is stronger in obese than normal-weight men. Int J Obes (Lond). 2016;40(11):1707-1714. DOI: 10.1038/ijo.2016.149.

[30] Newmaster KT, Nolan ZT, Chon U, Vanselow DJ, Weit AR, Tabbaa M,et al. Quantitative cellular-resolution map of the oxytocin receptor in postnatally developing mouse brains. Nat Commun. 2020;11(1):1885. DOI: 10.1038/s41467-020-15659-1.

[31] Welch MG, Tamir H, Gross KJ, Chen J, Anwar M, Gershon MD. Expression and developmental regulation of oxytocin (OT) and oxytocin receptors (OTR) in the enteric nervous system (ENS) and intestinal epithelium. J Comp Neurol. 2009;512(2):256-70. DOI: 10.1002/cne.21872.

[32] Yoshida M, Takayanagi Y, Inoue K, Kimura T, Young LJ, Onaka T, et al. Evidence that oxytocin exerts anxiolytic effects via oxytocin receptor expressed in serotonergic neurons in mice. J Neurosci. 2009;29(7):2259-71. DOI: 10.1523/JNEUROSCI.5593-08.2009.

[33] Neary NM, Small CJ, Druce MR, Park AJ, Ellis SM, Semjonous NM et al. Peptide YY3-36 and glucagon-like peptide-17-36 inhibit food intake additively. Endocrinology. 2005;146(12):5120-7. DOI: 10.1210/en.2005-0237.

[34] Maejima Y, Takahashi S, Takasu K, Takenoshita S, Ueta Y, Shimomura K. Orexin action on oxytocin neurons in the paraventricular nucleus of the hypothalamus. Neuroreport. 2017;28(6):360-366. DOI: 10.1097/WNR.0000000000000773.

[35] Maejima Y, Sedbazar U, Suyama S, Kohno D, Onaka T, Takano E, et al. Nesfatin-1-regulated oxytocinergic signaling in the paraventricular nucleus causes anorexia through a leptin-independent melanocortin pathway. Cell Metab. 2009;10(5):355-65. DOI: 10.1016/j.cmet.2009.09.002.

[36] Maejima Y, Kato S, Horita S, Ueta Y, Takenoshita S, Kobayashi K et al. The hypothalamus to brainstem circuit suppresses late-onset body weight gain. Sci Rep. 2019;9(1):18360. DOI: 10.1038/s41598-019-54870-z.

[37] Kerem L, Lawson EA. The Effects of Oxytocin on Appetite Regulation, Food Intake and Metabolism in Humans. Int J Mol Sci. 2021;22(14):7737. DOI: 10.3390/ijms22147737.

[38] Morton GJ, Cummings DE, Baskin DG, Barsh GS, Schwartz MW. Central nervous system control of food intake and body weight. Nature. 2006;443(7109):289-95. DOI: 10.1038/nature05026.

[39] Ten Kulve JS, van Bloemendaal L, Balesar R, IJzerman RG, Swaab DF, Diamant M, et al. Decreased Hypothalamic Glucagon-Like Peptide-1 Receptor Expression in Type 2 Diabetes Patients. J Clin Endocrinol Metab. 2016;101(5):2122-9. DOI: 10.1210/jc.2015-3291.

[40] Maejima Y, Sakuma K, Santoso P, Gantulga D, Katsurada K, Ueta Y, et al. Oxytocinergic circuit from paraventricular and supraoptic nuclei to arcuate POMC neurons in hypothalamus. FEBS Lett. 2014;588(23):4404-12. DOI: 10.1016/j.febslet.2014.10.010.

[41] Maejima Y, Yokota S, Nishimori K, Shimomura K. The anorexigenic neural pathways of oxytocin and their clinical implication. Neuroendocrinology. 2018;107(1):91-104. DOI: 10.1159/000489263.

[42] Bullitt E. Expression of c-fos-like protein as a marker for neuronal activity following noxious stimulation in the rat. J Comp Neurol. 1990;296(4):517-30. DOI: 10.1002/cne.902960402.

[43] Chung L. A Brief Introduction to the Transduction of Neural Activity into Fos Signal. Dev Reprod. 2015;19(2):61-7. DOI: 10.12717/DR.2015.19.2.061.

[44] Hicks C, Ramos L, Dampney B, Baracz SJ, McGregor IS, Hunt GE. Regional c-Fos expression induced by peripheral oxytocin administration is prevented by the vasopressin 1A receptor antagonist SR49059. Brain Res Bull. 2016;127:208-218. DOI: 10.1016/j.brainresbull.2016.10.005.

[45] Young LJ, Barrett CE. Neuroscience. Can oxytocin treat autism? Science. 2015;347(6224):825-6. DOI: 10.1126/science.aaa8120.

[46] Porter AG, Jänicke RU. Emerging roles of caspase-3 in apoptosis. Cell Death Differ. 1999;6(2):99-104. DOI: 10.1038/sj.cdd.4400476.

[47] Lee J, Moon H, Lee H, Oh Y, Kim C, Lee YH, et al. Antagonistic interaction between central glucagon-like Peptide-1 and oxytocin on diet-induced obesity mice. Heliyon. 2020;11;6(10):e05190. DOI: 10.1016/j.heliyon.2020.e05190.

[48] Leslie M, Silva P, Paloyelis Y, Blevins J, Treasure J. A Systematic Review and Quantitative Meta-Analysis of Oxytocin's Effects on Feeding. J Neuroendocrinol. 2018:10.1111/jne.12584. DOI: 10.1111/jne.12584.

[49] Kublaoui BM, Gemelli T, Tolson KP, Wang Y, Zinn AR. Oxytocin deficiency mediates hyperphagic obesity of Sim1 haploinsufficient mice. Mol Endocrinol. 2008;22(7):1723-34. DOI: 10.1210/me.2008-0067.

[50] Johnstone LE, Fong TM, Leng G. Neuronal activation in the hypothalamus and brainstem during feeding in rats. Cell Metab. 2006;4(4):313-21. DOI: 10.1016/j.cmet.2006.08.003.

[51] Zhang G, Cai D. Circadian intervention of obesity development via resting-stage feeding manipulation or oxytocin treatment. Am J Physiol Endocrinol Metab. 2011;301(5):E1004-12. DOI: 10.1152/ajpendo.00196.2011.

[52] Qian W, Zhu T, Tang B, Yu S, Hu H, Sun W et al. Decreased circulating levels of oxytocin in obesity and newly diagnosed type 2 diabetic patients. J Clin Endocrinol Metab. 2014;99(12):4683-9. DOI: 10.1210/jc.2014-2206. PMID: 25233153.

[53] Yuan G, Qian W, Pan R, Jia J, Jiang D, Yang Q et al. Reduced circulating oxytocin and High-Molecular-Weight adiponectin are risk factors for metabolic syndrome. Endocr J. 2016;63(7):655-62. DOI: 10.1507/endocrj.EJ16-0078.

[54] Blevins JE, Schwartz MW, Baskin DG. Evidence that paraventricular nucleus oxytocin neurons link hypothalamic leptin action to caudal brain stem nuclei controlling meal size. Am J Physiol Regul Integr Comp Physiol. 2004;287(1):R87-96. DOI: 10.1152/ajpregu.00604.2003.

[55] Ong ZY, Bongiorno DM, Hernando MA, Grill HJ. Effects of Endogenous Oxytocin Receptor Signaling in Nucleus Tractus Solitarius on Satiation-Mediated Feeding and

Thermogenic Control in Male Rats. Endocrinology. 2017;158(9):2826-2836. DOI: 10.1210/en.2017-00200.

[56] Takayanagi Y, Kasahara Y, Onaka T, Takahashi N, Kawada T, Nishimori K. Oxytocin receptor-deficient mice developed late-onset obesity. Neuroreport. 2008;19(9):951-5. DOI: 10.1097/WNR.0b013e3283021ca9.

[57] Camerino C. Low sympathetic tone and obese phenotype in oxytocin-deficient mice. Obesity (Silver Spring). 2009;17(5):980-4. DOI: 10.1038/oby.2009.12.

[58] Camerino C. The New Frontier in Oxytocin Physiology: The Oxytonic Contraction. Int J Mol Sci. 2020;21(14):5144. DOI: 10.3390/ijms21145144.

[59] Amico JA, Vollmer RR, Cai HM, Miedlar JA, Rinaman L. Enhanced initial and sustained intake of sucrose solution in mice with an oxytocin gene deletion. Am J Physiol Regul Integr Comp Physiol. 2005;289(6):R1798-806. DOI: 10.1152/ajpregu.00558.2005.

[60] Baggio LL, Drucker DJ. Glucagon-like peptide-1 receptors in the brain: controlling food intake and body weight. J Clin Invest. 2014;124(10):4223-6. DOI: 10.1172/JCI78371.

[61] Meeran K, O'Shea D, Edwards CM, Turton MD, Heath MM, Gunn I, et al. Repeated intracerebroventricular administration of glucagon-like peptide-1-(7-36) amide or exendin-(9-39) alters body weight in the rat. Endocrinology. 1999;140(1):244-50. DOI: 10.1210/endo.140.1.6421.

[62] Barrera JG, Jones KR, Herman JP, D'Alessio DA, Woods SC, Seeley RJ. Hyperphagia and increased fat accumulation in two models of chronic CNS glucagon-like peptide-1 loss of function. J Neurosci. 2011;31(10):3904-13. DOI: 10.1523/JNEUROSCI.2212-10.2011.

[63] Kanoski SE, Hayes MR, Skibicka KP. GLP-1 and weight loss: unraveling the diverse neural circuitry. Am J Physiol Regul Integr Comp Physiol. 2016;310(10):R885-95. DOI: 10.1152/ajpregu.00520.2015. Epub 2016 Mar 30.

[64] Drucker DJ. GLP-1 physiology informs the pharmacotherapy of obesity. Mol Metab. 2022;57:101351. DOI: 10.1016/j.molmet.2021.101351.

[65] Schwartz MW, Woods SC, Porte D Jr, Seeley RJ, Baskin DG. Central nervous system control of food intake. Nature. 2000;404(6778):661-71. DOI: 10.1038/35007534.

[66] Cone RD. Anatomy and regulation of the central melanocortin system. Nat Neurosci. 2005 ;8(5):571-8. DOI: 10.1038/nn1455.

[67] Blackshaw LA, Grundy D, Scratcherd T. Involvement of gastrointestinal mechano- and intestinal chemoreceptors in vagal reflexes: an electrophysiological study. J Auton Nerv Syst. 1987;18(3):225-34. DOI: 10.1016/0165-1838(87)90121-4.

[68] Mens WB, Witter A, van Wimersma Greidanus TB. Penetration of neurohypophyseal hormones from plasma into cerebrospinal fluid (CSF): half-times of disappearance of these neuropeptides from CSF. Brain Res. 1983;262(1):143-9. DOI: 10.1016/0006-8993(83)90478-x.

[69] Yamamoto Y, Liang M, Munesue S, Deguchi K, Harashima A, Furuhara K, et al. Vascular RAGE transports oxytocin into the brain to elicit its maternal bonding behaviour in mice. Commun Biol. 2019;2:76. DOI: 10.1038/s42003-019-0325-6.

[70] Kastin AJ, Akerstrom V, Pan W. Interactions of glucagon-like peptide-1 (GLP-1) with the blood-brain barrier. J Mol Neurosci. 2002;18(1-2):7-14. DOI: 10.1385/JMN:18:1-2:07.

[71] Hauge M, Ekberg JP, Engelstoft MS, Timshel P, Madsen AN, Schwartz TW. Gq and Gs signaling acting in synergy to control GLP-1 secretion. Mol Cell Endocrinol. 2017;449:64-73. DOI: 10.1016/j.mce.2016.11.024.

[72] Marzook A, Tomas A, Jones B. The Interplay of Glucagon-Like Peptide-1 Receptor Trafficking and Signalling in Pancreatic Beta Cells. Front Endocrinol (Lausanne). 2021;12:678055. DOI: 10.3389/fendo.2021.678055.

[73] Yuan S, Xia L, Wang C, Wu F, Zhang B, Pan C et al. Conformational Dynamics of the Activated GLP-1 Receptor-Gs Complex Revealed by Cross-Linking Mass Spectrometry and Integrative Structure Modeling. ACS Cent Sci. 2023;9(5):992-1007. DOI: 10.1021/acscentsci.3c00063.

[74] Jurek B, Neumann ID. The Oxytocin Receptor: From Intracellular Signaling to Behavior. Physiol Rev. 2018;98(3):1805-1908. DOI: 10.1152/physrev.00031.2017.

[75] Wu Z, Xu Y, Zhu Y, Sutton AK, Zhao R et al. An obligate role of oxytocin neurons in diet induced energy expenditure. PLoS One. 2012;7(9):e45167. DOI: 10.1371/journal.pone.0045167.

[76] Xi D, Long C, Lai M, Casella A, O'Lear L, Kublaoui B et al. Ablation of Oxytocin Neurons Causes a Deficit in Cold Stress Response. J Endocr Soc. 2017;1(8):1041-1055. DOI: 10.1210/js.2017-00136.

Figure legends

Fig.1 Cumulative food intake after intraperitoneal (IP) injection of GLP-1, OXT and co-administration of OXT and GLP-1 in lean mice.

A; Food intake at 0.5, 1, 2, 3, 6 and 24 hours after IP injection of control saline, 50 μg/kg GLP-1 and 100 μg/kg GLP-1. *n* = 8, 8, 7 in control, 50 μg/kg GLP-1 and 100 μg/kg GLP-1, respectively. **B**; Food intake at 0.5, 1, 2, 3, 6 and 24 hours after IP injection of control saline, 100 μg/kg OXT and 200 μg/kg OXT. *n* = 6, 7, 7 in control, 100 μg/kg OXT and 200 μg/kg OXT, respectively. **C**; Food intake at 0.5, 1, 2, 3, 6 and 24 hours after IP injection of control saline, 200 μg/kg OXT, 100 μg/kg GLP-1 and 200 μg/kg OXT plus100 μg/kg GLP-1. *n* = 12, 10, 12, 11 in control, 200 μg/kg OXT and 100 μg/kg GLP-1 and 200 μg/kg OXT plus100 μg/kg GLP-1, respectively. The food intake at 24 h was 4.18 ±0.17, 3.75 ±0.17, 3.74 ±0.19 and 3.30 ± 0.21 g, in control, OXT, GLP-1 and OXT/GLP-1 group, respectively. *P < 0.05, **P < 0.01. Repeated measures two-way ANOVA followed by Tukey's multiple range test. All data shown as mean ± SEM.

Fig.2 c-Fos expression in the brain after intraperitoneal (IP) injection of GLP-1, OXT and co-administration of OXT and GLP-1 in lean mice.

A; The representative image of c-Fos distribution in paraventricular nucleus (PVN), arcuate nucleus (ARC), supraoptic nucleus (SON) and dorsal vagal complex (nucleus tractus solitarius (NTS)/ area postrema (AP)/dorsal motor nucleus of the vagus (DMNV)). Control, OXT (200 μg/kg), GLP-1(100 μg/kg) and co-administration of OXT and GLP-1 from left to right column, respectively. 3V: 3rd ventricle, OC: optic chiasm. Scales =

100 μm. **B-G;** The number of c-Fos positive neurons per section in the PVN (A), ARC (B), SON (C), NTS (D), AP (F) and DMNV (G) in each group. $n = 4$ in each group in all graph. *P < 0.05, One-way ANOVA followed by Tukey's multiple range test. All data shown as mean ± SEM.

Fig.3 c-Fos expression in the OXT neurons after intraperitoneal (IP) injection of GLP-1, OXT and co-administration of OXT and GLP-1 in lean mice.

A-D; Representative image of double immunostaining of c-Fos and OXT in the PVN after IP injection of control saline (A), 200 μg/kg OXT (B), 100 μg/kg GLP-1(C) and co-administration of OXT and GLP-1(D). Scale = 100 μm. Bottom right insets represent enlargements of the areas in dotted squares. Black arrow heads indicate the double immune-stained c-Fos and OXT. scale bars = 10μm. **E, F;** The percentage of OXT neurons in active (c-Fos expressed) neurons in the PVN (E) and SON (F) in each group. $n = 4$ in each group in both graphs. *P < 0.05, **P < 0.01. One-way ANOVA followed by Tukey's multiple range test. All data shown as mean ± SEM. **G, H;** The percentage of active (c-Fos expressed) neurons in OXT neurons in the PVN (G) and SON (H) in each group. $n = 4$ in each group in both graphs. *P < 0.05, **P < 0.01. One-way ANOVA followed by Tukey's multiple range test. All data shown as mean ± SEM.

Fig. 4 Distribution of OXTR, GLP-1R and OXT in the PVN of OXTR-Venus male mice.

A; The representative image of OXTR (i), GLP-1R (ii) and Merged image (iii). Scale bars = 100 μm. Bottom right images represent enlargements of the areas in dotted squares. White arrow heads indicate double labeled neuron with OXTR and GLP-1R. Scale bars

= 10 μm. **B;** The summary of GLP-1R positive neuronal population in the PVN. In GLP-1R positive neurons, 68.6% were OXTR positive, 31.4% were OXTR negative. *n* = 4. **C;** The representative image of OXTR (i), OXT (ii) and merged image (iii). Scale bars = 100 μm. Bottom right images represent enlargements of the areas in dotted squares. White arrow heads indicate double labeled neuron with OXTR and OXT. Scale bars = 10 μm. **D;** The summary of OXT positive neuronal population in the PVN. In OXT positive neurons, 53.1% were OXTR positive, and 46.9% were OXTR negative. *n* = 3.

Fig.5 The effect of dual treatment of OXT and GLP-1 on the membrane potential and firing frequency in the OXTR positive neurons in the PVN.

A-C; Representative membrane potential recording from identified OXTR positive neurons under treatment of 10^{-10} M OXT (A), 10^{-10} M GLP-1 (B) and co-administration of OXT and GLP-1 (C) in brain slice patch clamp. **D;** Mean delta membrane potential from control. 2.13 ±1.1 mV for OXT, 5.5 ± 2.17 mV for GLP-1, 10.39 ± 2.48 mV for OXT and GLP-1. *n* = 7 in each group. **E;** Mean firing frequency in each group. 0.03 ± 0.03 Hz for control, 0.15 ± 0.1 Hz for OXT, 0.16 ± 0.13 Hz for GLP-1, 4.89 ± 2.27 Hz for OXT and GLP-1. *n* = 6 in each group. *P < 0.05, One-way ANOVA followed by Tukey's multiple range test. All data shown as mean ± SEM.

Fig.6 The effect of dual treatment of OXT and GLP-1 on cytosolic Ca^{2+} $[Ca^{2+}]_i$ in the PVN neurons.

A-C; Representative recording of $[Ca^{2+}]_i$ in the neurons isolated from PVN with administration of 10^{-14} M GLP-1 (A), 10^{-12} M GLP-1 (B) and 10^{-10} M GLP-1 (C). **D;** The mean of peak amplitude in during 5 mins of each dose of GLP-1 administration. *n* = 90,

12, 16, and 19 in control, 10^{-14} M GLP-1, 10^{-12} M GLP-1 and 10^{-10} M GLP-1, respectively. *P < 0.05, One-way ANOVA followed by Tukey's multiple range test. The data shown as mean ± SEM. **E-G;** Representative recording of $[Ca^{2+}]_i$ in the neurons isolated from PVN under administration of 10^{-14} M OXT (E), 10^{-12} M OXT (F) and 10^{-10} M OXT (G). **H;** The mean of peak amplitude in during 5 mins of each dose of OXT administration. *n* = 14, 23, 25, and 19 in control, 10^{-14} M OXT, 10^{-12} M OXT and 10^{-10} M OXT, respectively. *P < 0.05, One-way ANOVA followed by Tukey's multiple range test. The data shown as mean ± SEM. **I;** Representative recording of $[Ca^{2+}]_i$ in the OXT neurons under sequential administration of 10^{-12} M OXT, 10^{-12} M GLP-1 and co-administration of OXT and GLP-1. This data was recorded from OXT neurons, as identified in the image in the upper right panel. Scale bar = 10 μm. **J;** The mean of peak amplitude in during 5 mins of each dose of OXT administration, GLP-1 at and co-administration of OXT and GLP-1. Right bar graph (red bar) indicates the mean of peak amplitude during10 mins after beginning of co-administration of OXT and GLP-1. *n* = 10 in each group. *P < 0.05, **P < 0.01, One-way ANOVA followed by Tukey's multiple range test. The data shown as mean ± SEM. **K;** Area under the curve (AUC) of $[Ca^{2+}]_i$ for 0-5 min (5 min) and 5-10 min (5 min) in co-administration of OXT and GLP-1. *n* = 10, *P < 0.05, paired t-test.

Fig. 7 The effect of dual treatment of OXT and GLP-1 on body weight (BW) change, food intake and blood glucose in high fat diet (HFD)- fed mice.

A, B; BW change (A) and food intake (B) after beginning of each treatment (control; saline, OXT; 400 μg/kg/day, GLP-1; 200 μg/kg/day, OXT/GLP-1; 400 μg OXT/ 200 μg GLP-1/kg/day) by osmotic minipump. *n* = 4, 5, 5, 5 in control, OXT, GLP-1 and OXT/GLP-1 group, respectively. *#P < 0.05, **P < 0.01, Repeated measures two-way

ANOVA followed by Tukey's multiple range test. * means vs. Control. # means vs. GLP-1 group. The data shown as mean ± SEM. **C;** Food efficacy to BW gain (BW gain / amount of food intake) after 7 -13 days of beginning to diffuse each peptide. n = 4, 5, 5, 5 in control, OXT, GLP-1 and OXT/GLP-1 group, respectively. *P < 0.05, **P < 0.01. Repeated measures two-way ANOVA followed by Tukey's multiple range test. The data shown as mean ± SEM. **D;** Percentage of BW change at day 13 from initial BW. 5.0 ± 1.2% for control, 0.3 ± 0.7% for OXT, 1.5 ± 0.9% for GLP-1, and -4.0 ± 2.7% for co-administration of OXT and GLP-1. n = 4, 5, 5, 5 in control, OXT, GLP-1 and OXT/GLP-1 group, respectively. *P < 0.05, One-way ANOVA followed by Tukey's multiple range test. The data shown as mean ± SEM. **E;** Total food intake in each group for 13 days. 43.6 ± 1.4 g for control, 42.0 ± 1.9 g for OXT, 40.0 ± 1.5 g for GLP-1 and 38.9 ± 2.6 g for co-administration of OXT and GLP-1. n = 4, 5, 5, 5 in control, OXT, GLP-1 and OXT/GLP-1 group, respectively. One-way ANOVA followed by Tukey's multiple range test. These are no significant difference among these groups. The data shown as mean ± SEM. **F;** 2 h-fasting blood glucose at day 14. 173.8 ± 7.3 g/dl for control, 180.2 ± 5.7 g/dl for OXT, 157.8 ± 9.4 g/dl for GLP-1, and 159.0 ± 13.4 g/dl for co-administration of OXT and GLP-1. n = 4, 5, 5, 5 in control, OXT, GLP-1 and OXT/GLP-1 group, respectively. One-way ANOVA followed by Tukey's multiple range test. These are no significant difference among these groups. The data shown as mean ± SEM. **G;** Plasma OXT level at day 14. 62.7 ± 17.6 pg/ml for control, 1683.2 ± 310.4 pg/ml for OXT, 287.7 ± 135.2 pg/ml for GLP-1 and 2075.5 ± 276.5 pg/ml for co-administration of OXT and GLP-1. n = 6, 5, 5, 5 in control, OXT, GLP-1 and OXT/GLP-1 group, respectively. ** P < 0.01, One-way ANOVA followed by Tukey's multiple range test.

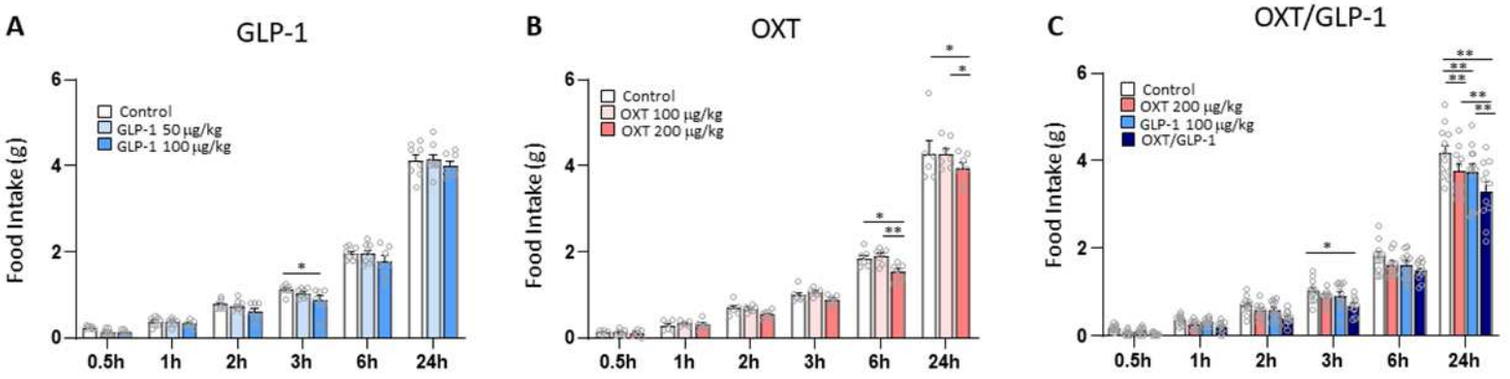

Figure1. Maejima et al

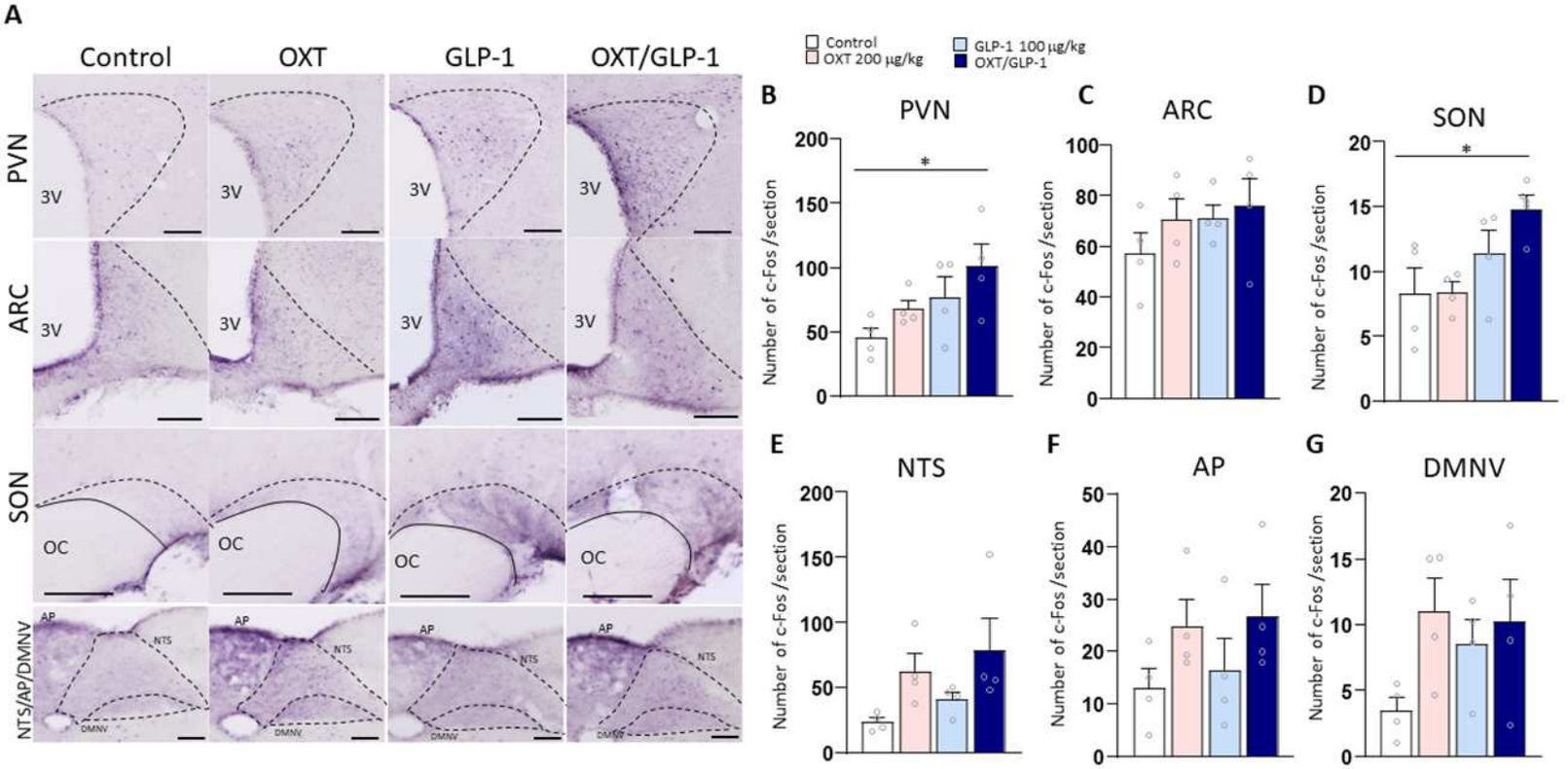

Figure2. Maejima et al

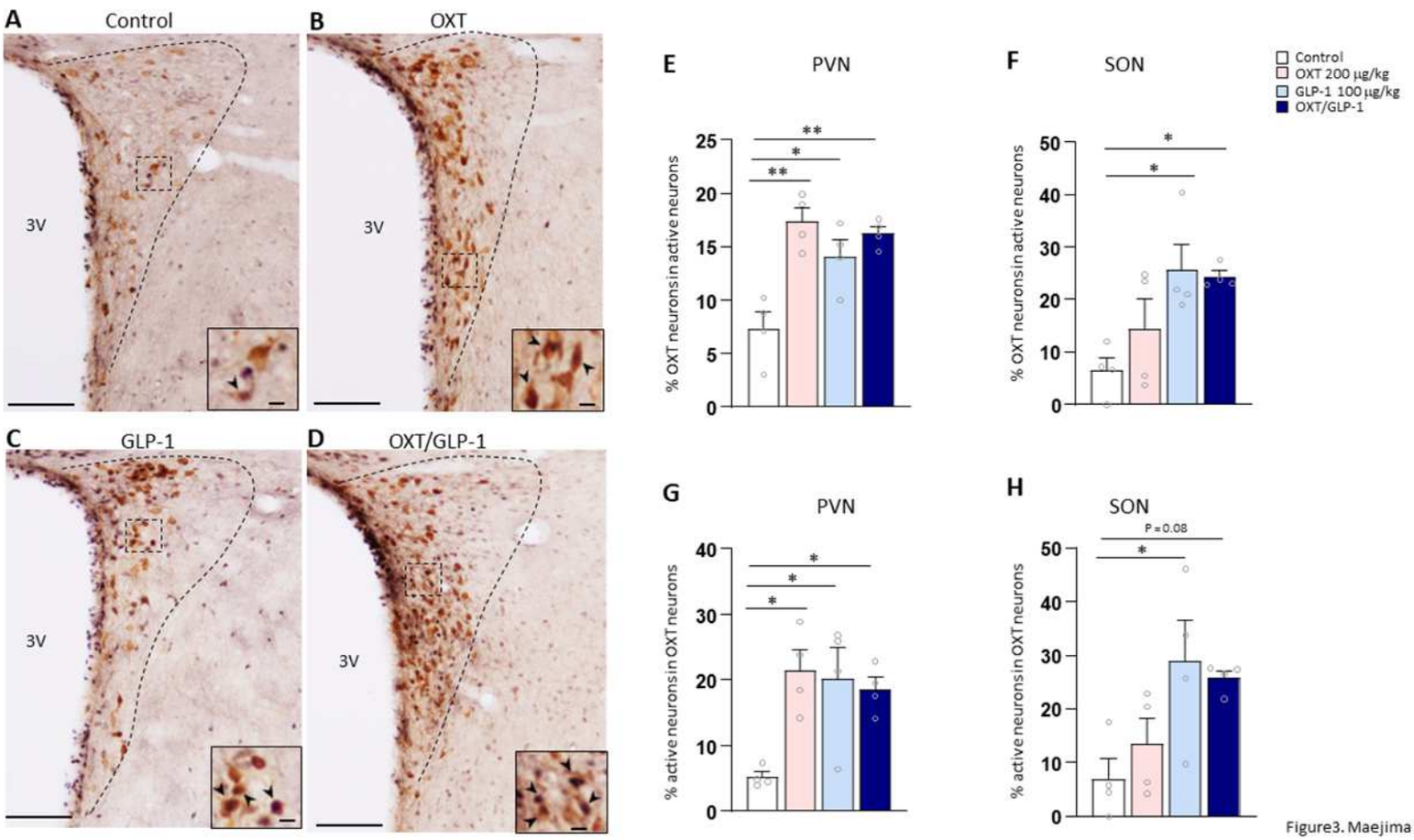

Figure3. Maejima et al

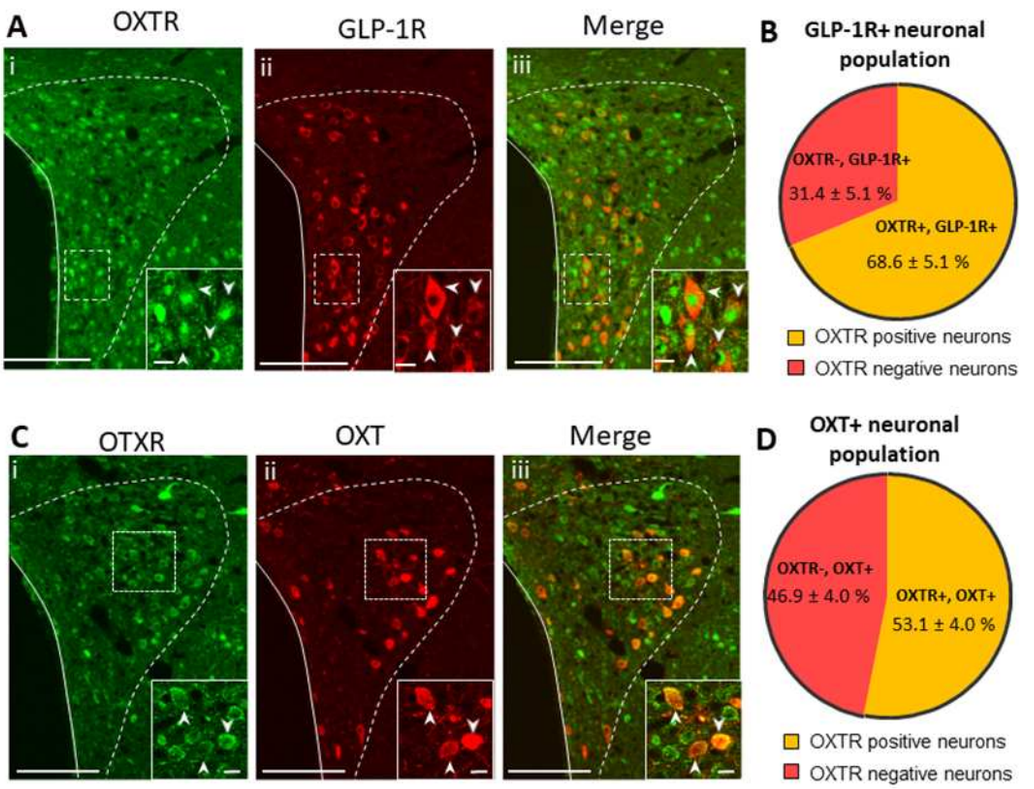

Figure4. Maejima et al

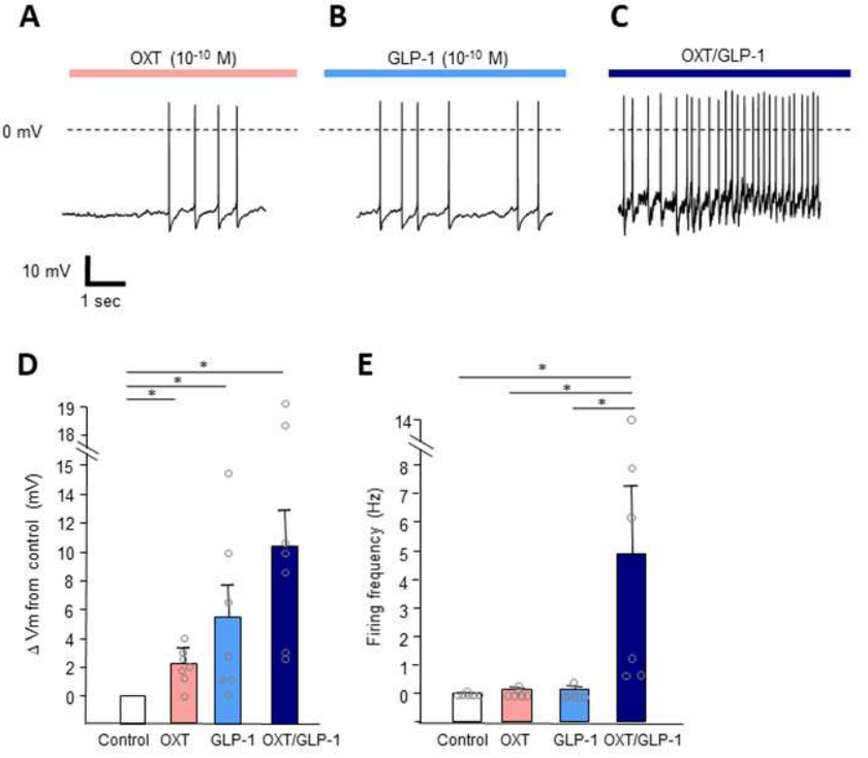

Figure5. Maejima et al

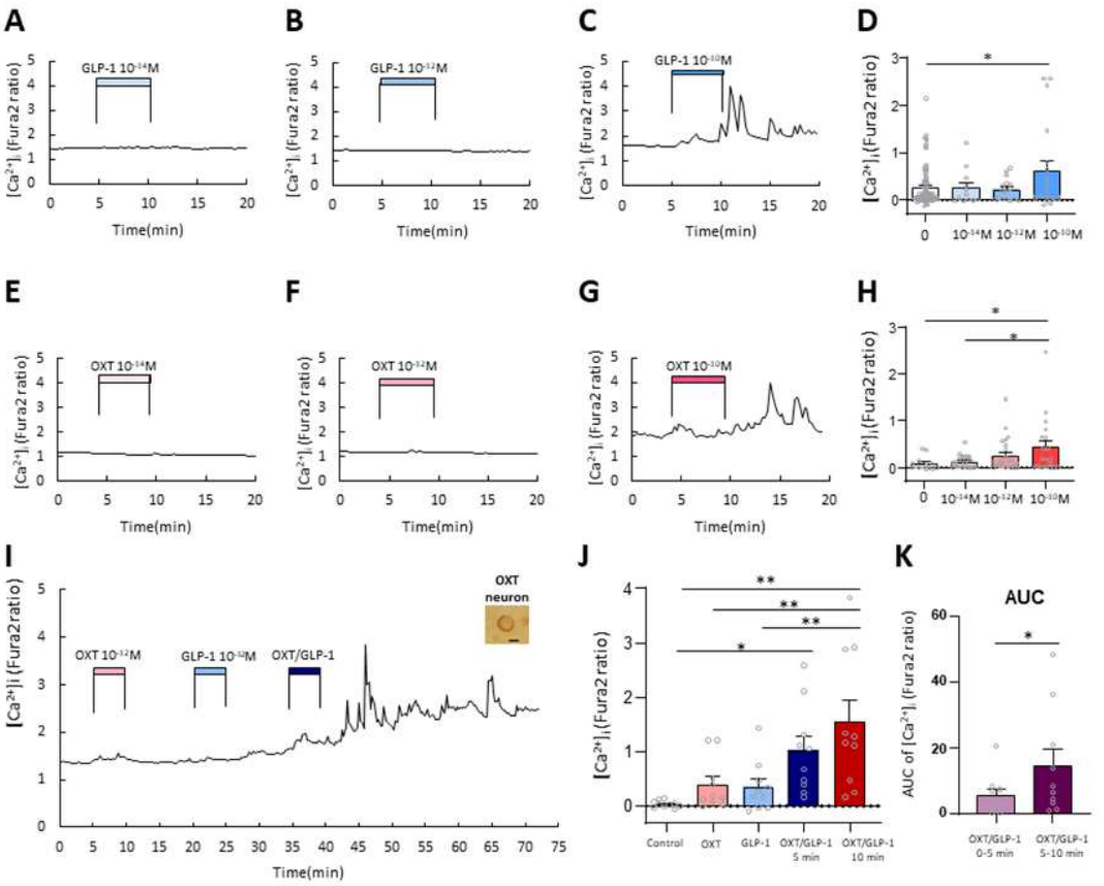

Figure6. Maejima et al

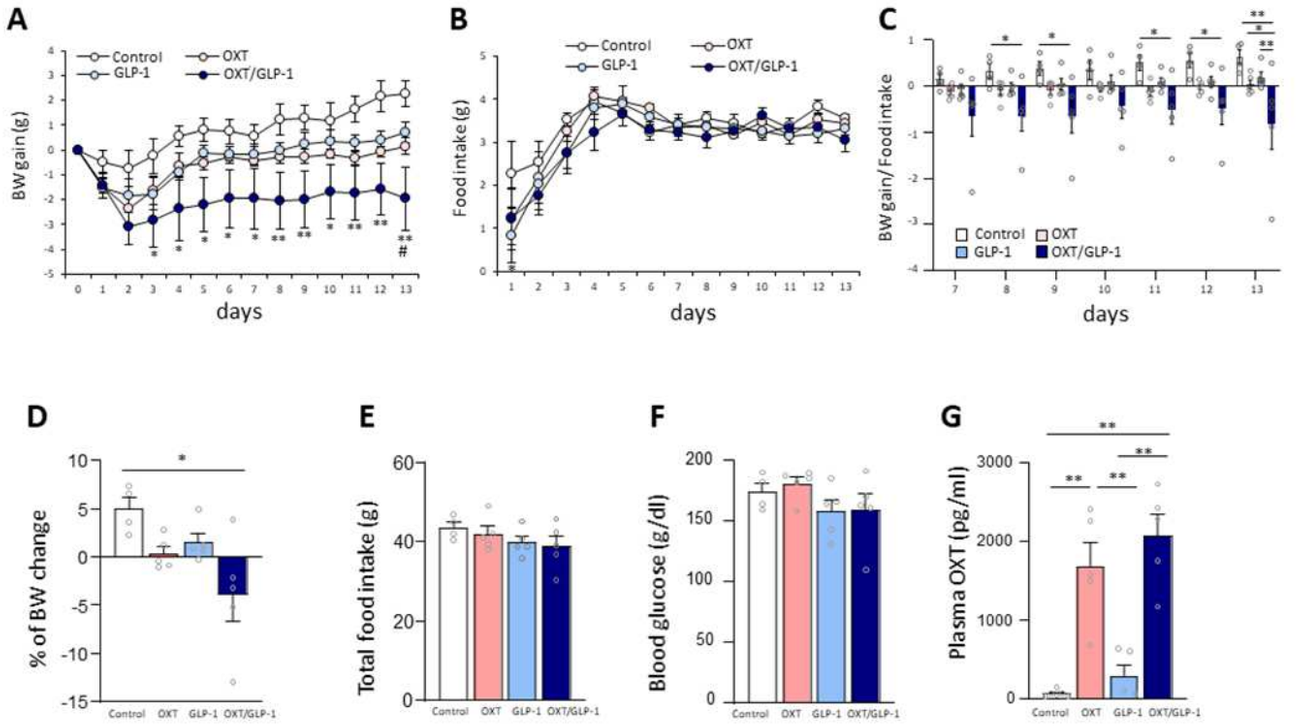

Figure7. Maejima et al

Supplemental Information

Systemic co-administration of low dose oxytocin and glucagon like peptide-1 additively decreases food intake and body weight

Yuko Maejima[1,2,3], Shoko Yokota[1], Shizu Hidema[1], Katsuhiko Nishimori[2], Heidi de Wet[3], Kenju Shimomura[1, 2]

[1]*Department of Bioregulation and Pharmacological Medicine, Fukushima Medical University School of Medicine, Fukushima-shi, 960-1295, Fukushima, Japan*

[2]*Departments of Obesity and Inflammation Research, Fukushima Medical University School of Medicine, Fukushima-shi, 960-1295, Fukushima, Japan*

[3]*Department of Physiology, Anatomy and Genetics, Sherrington Building, University of Oxford, United Kingdom*

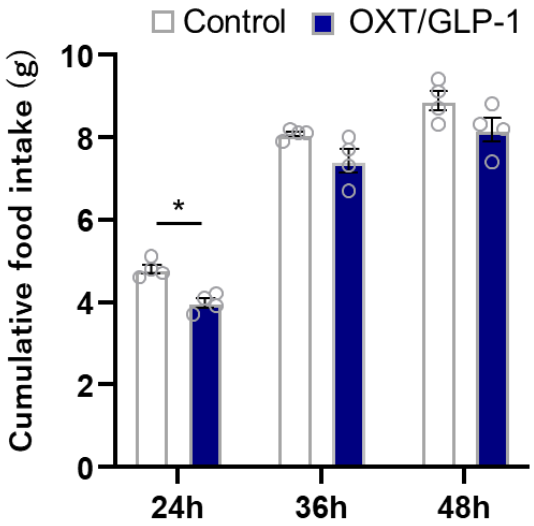

Supplemental figure 1. Cumulative food intake after co-administration of OXT and GLP-1 by intraperitoneal (IP) injection of lean mice.

Eight 12-week-old male C57BL/6J mice (purchased from Japan SLC (Japan) were divided into two groups ($n = 4, 4$) (BW; control:26.3 ± 1.0 g OXT/GLP-1: 25.7 ± 0.7 g) and, used for food intake measurement after intraperitoneal (IP) injection of GLP-1 and OXT, at 24h, 36h and 48h. There were no significant differences in cumulative food intake in the control and OXT/GLP-1 groups at 36 h. *$P < 0.05$, Repeated measures two-way ANOVA followed by Tukey's multiple range test. Data shown as mean ± SEM.

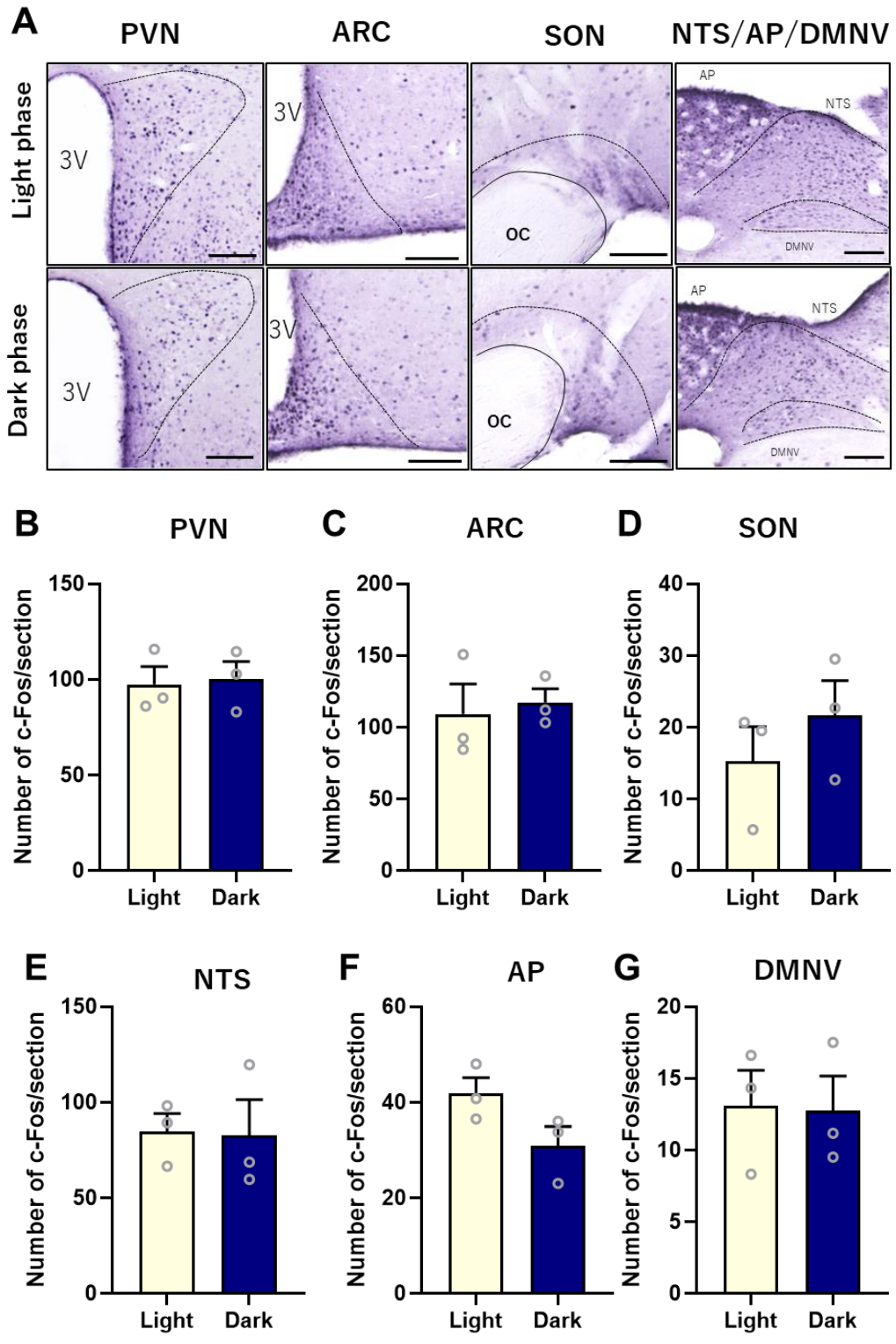

Supplemental figure 2. Light phase and dark phase comparison of c-Fos expression in the brain after co-administration of OXT and GLP-1 via intraperitoneal (IP) injection.

Six 12-week-old male C57BL/6J mice (purchased from Japan SLC (Japan) were divided into two groups (n = 3, 3) (BW; light phase:27.2 ± 0.8 g, dark phase: 26.8 ± 0.8 g) and, used for immunohistochemistry for c-Fos.

In the light phase group, food was removed at 9:00, and OXT/GLP-1 (OXT 200 and GLP-1 100 μg/kg/5ml) were IP injected at 11:00. After 2h, animals were IP injected with a mixture of three types of anesthetic agents and perfused intracardially with 4% paraformaldehyde (PFA) and 0.2% picric acid (light phase group).

In the dark phase group, food was removed at 17:00, and OXT/GLP-1 (OXT 200 and GLP-1 100 μg/kg/5ml) were IP injected at 19:00. After 2h, animals were IP injected with a mixture of three types of anesthetic agents and perfused intracardially with 4% paraformaldehyde (PFA) and 0.2% picric acid (dark phase group). The methods for staining and analysis for c-Fos were same as "c-Fos immunostaining after IP injection of GLP-1 and OXT" in the method section, described in main text.

A;The representative image of c-Fos distribution in paraventricular nucleus (PVN), arcuate nucleus (ARC), supraoptic nucleus (SON) and dorsal vagal complex (nucleus tractus solitarius (NTS)/ area postrema (AP)/dorsal motor nucleus of the vagus (DMNV) in light phase (upper row) and dark phase (bottom row).

G-G; There were no differences in c-Fos expression after OXT/GLP-1 injection in PVN (A, B), ARC (A, C), SON (A, D), NTS/AP/DMNV (A, E-G) between the light phase and dark phase.

3V: 3rd ventricle, OC: optic chiasm. Scales = 100 μm. n = 3 in each group in all graph. All data shown as mean ± SEM. n.s; no significant differences. Unpaired t-test.

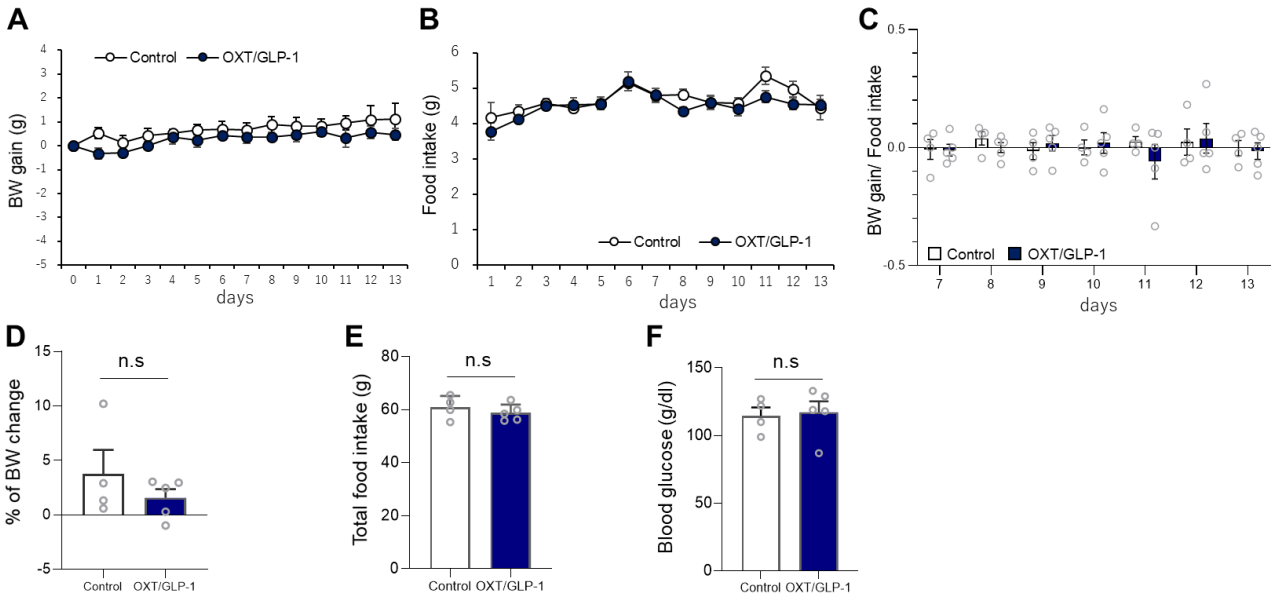

Supplemental figure 3.

The effect of dual treatment of OXT and GLP-1 on body weight (BW) change, food intake and blood glucose on standard chow- fed lean mice.

Nine C57BL/6J male mice (14 weeks old), fed with standard chow were divided into two groups (control n = 4, OXT/GLP-1 n =5). These mice were anesthetized by a mixture of three types of anesthetic agents (10 ml/kg) and osmotic mini-pumps were surgically implanted (Alzet; model 2002 for 14days, CA) subcutaneously at the back. Osmotic mini-pumps contained control saline or OXT/GLP-1(400 μg/kg/day, 200 μg/kg/day, respectively). The concentration of OXT and GLP-1 was calculated from individual BW, and each solution was filled into each osmotic minipump. Food and BW were measured every day at 17:00 (2 hours before the onset of the dark phase) for 13 days. Initial BW were 31.1 ± 0.96 g and 31.3 ± 1.03 g in control and OXT/GLP- group, respectively.

A, B; BW change (A) and food intake (B) after beginning of each treatment (control; saline, OXT/GLP-1; 400 μg OXT/ 200 μg GLP-1/kg/day) by osmotic minipump. n = 4, 5 in control and OXT/GLP-1 group, respectively. Repeated measured two-way ANOVA followed by Tukey's multiple range test. There were no significant differences in BW and food intake at any time points. The data shown as mean ± SEM. **C;** Food efficacy to BW gain (BW gain / amount of food intake) after 7 -13 days of commencement of peptide diffusion. n = 4, 5 in control and OXT/GLP-1 group, respectively. Repeated measured two-way ANOVA followed by Tukey's multiple range test. The data shown as mean ± SEM. There were no significant differences in BW and food intake at any time points. **D;**

Percentage of BW change at day 13 from initial BW. 3.8 ± 2.2% for control and 1.6 ± 0.8% for co-administration of OXT and GLP-1. n = 4, 5 in control and OXT/GLP-1 group, respectively. n.s; no significant differences in these two group. unpaired t-test. **E;** Total food intake in each group for 13 days. 60.9 ± 2.2 g for control and 58.8 ± 1.4 g for co-administration of OXT and GLP-1. n = 4, 5 in control, and OXT/GLP-1 group, respectively. n.s; no significant differences in these two group. unpaired t-test. **F;** 2 h-fasting blood glucose at day 14. 114.5 ± 6.3 g/dl for control and 117.2 ± 8.1 g/dl for co-administration of OXT and GLP-1. n = 4, 5 in control, OXT/GLP-1 group, respectively. n.s; no significant differences in these two group. unpaired t-test.

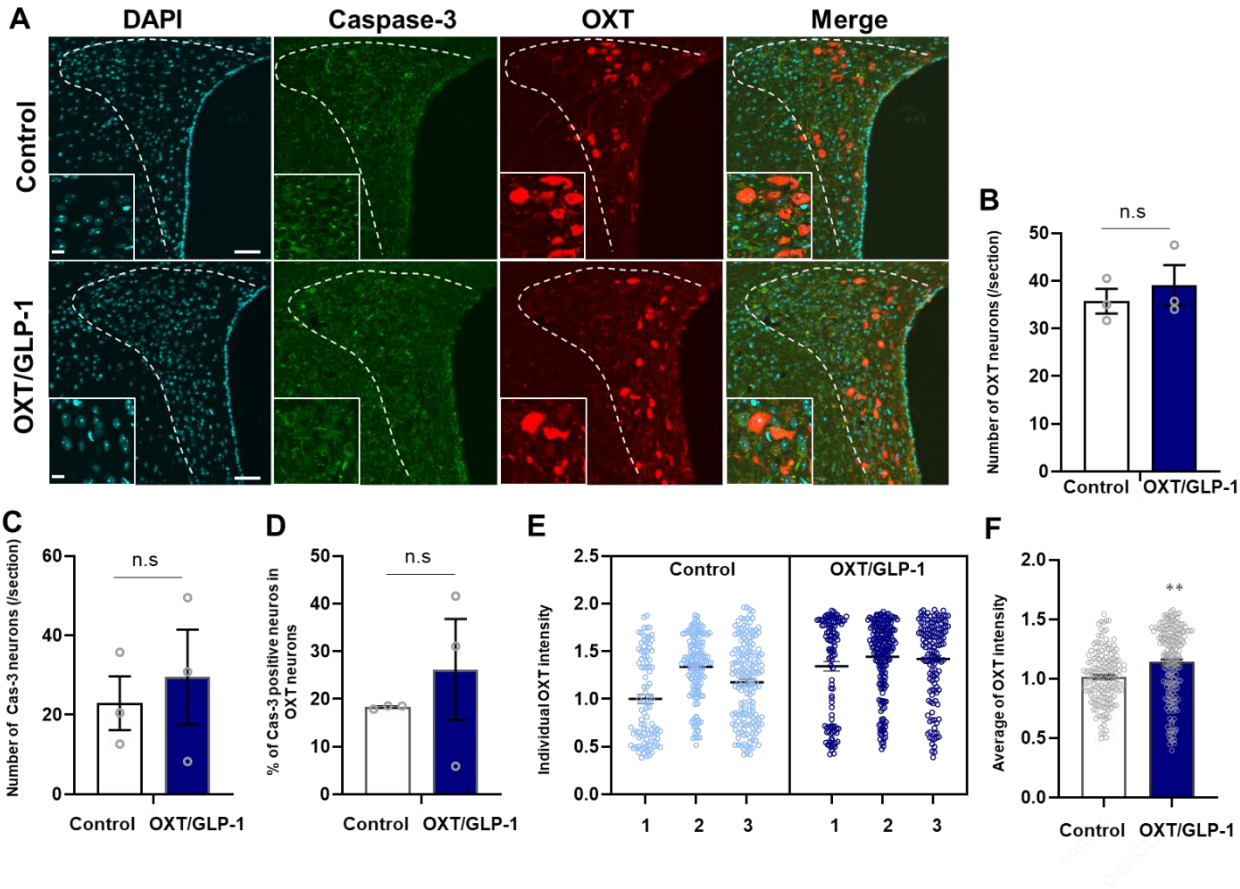

Supplemental figure 4. The analysis of OXT neurons in the PVN after sub-chronic OXT/GLP-1 treatment.

Six C57BL/6J male mice (14 weeks old), fed standard chow were divided into two group (control n = 3, OXT/GLP-1 n =3). These mice were anesthetized by a mixture of three types of anesthetic agents (10 ml/kg) and osmotic minipumps were surgically implanted (Alzet; model 2002 for 14days, CA) subcutaneously in the back. Osmotic mini-pumps contained saline for the controls or OXT/GLP-1(400 μg/kg/day, 200 μg/kg/day, respectively). The concentration of OXT and GLP-1 was calculated from individual BW, and each solution was filled into each osmotic minipump. At Day14, these mice were anesthetized by a mixture of three types of anesthetic agents (10 ml/kg) and perfused intracardially with 4% paraformaldehyde (PFA) and 0.2% picric acid. Serial coronal sections (40 μm thick) were collected from each mouse using a freezing microtome. The PVN containing sections at 120 μm intervals between -0.58 mm and −1.22 mm from the bregma were used for immunostaining. Thus, 4-5 sections from one mouse were used for immunostaining. The sections were washed in PBS and incubated for 1 h in a blocking solution comprising of 0.1% TritonX-100, 2% BSA, and 5% normal goat serum (NGS).

The sections were incubated with rabbit anti-OXT antibody (1:1000; 20068, ImmunoStar, WI) and with mouse anti-active caspase 3 antibody (1:400; bsm-33199M, Bioss, MA) in blocking solution overnight at 4 °C. Then sections were incubated with Alexa flour 594-labelled goat anti rabbit IgG (1:400, Life Technologies, CA) and, Alexa flour 488-labelled goat anti mouse IgG (1:400, Life Technologies, CA) for 40 min. Sections were mounted on glass slides and covered. Confocal fluorescence images were acquired in same fluorescence condition and OXT positive neurons and caspase 3 positive neurons and double positive neurons were counted. The intensity of fluorescence in OXT neurons are analyzed from confocal images by using Image J software.

A; Representative image the staining caspase 3 (Cas3) and OXT neurons in control group (upper row) and OXT/GLP-1 treated group (bottom row). Scale = 50 μm. The images in left bottom indicate enlarged images. Scale = 10 μm.
B; The number of OXT positive neurons per section. n.s; no significant differences. Unpaired t-test. (n = 3).
C; The number of caspase 3 positive neurons per section. n.s; no significant differences. Unpaired t-test. (n = 3).
D; The percentage of caspase 3 positive neurons in OXT positive neurons. n.s; no significant differences. Unpaired t-test. (n = 3).
E; OXT fluorescence intensity in each OXT neurons from individual 6 mice. The average of fluorescence intensity in control #1 mouse was corrected to 1. (control1-3: n = 95, 140, 162, respectively, OXT/GLP-1 1-3: n = 109, 190, 136, respectively.)
F; The average of OXT fluorescence intensity in control and OXT/GLP-1 group. The average of fluorescence intensity in control group was corrected to 1. ** $P < 0.05$, Unpaired t-test. (control: n = 397, OXT/GLP-1: n = 435).